

MODEST24

# Investigating Blue Straggler Stars of Open Clusters and Fields using AstroSat/UVIT



Kaushar Vaidya

Department of Physics, Birla Institute of Technology and Science Pilani

In collaboration with

**Anju Panthi**

**Vikrant Jadhav**

**Annapurni Subramaniam**

**Nagraj Vernekar**

**Manan Agarwal**

**Khushboo K. Rao**

**Sindhu Pandey**

**Sharmila Rani**

**Sivarani Tirupathi**

**Saketh Pinapati**



**BITS Pilani**  
Pilani | Dubai | Goa | Hyderabad



UNIVERSITY  
OF AMSTERDAM



**aries**  
आर्यभट्ट प्रेक्षण विज्ञान शोध संस्थान  
Aryabhata Research Institute of Observational Sciences

# UVIT Open Cluster Study (UOCS)



## UOCS – VII. Blue straggler populations of open cluster NGC 7789 with UVIT/AstroSat

Kaushar Vaidya<sup>1</sup>,<sup>1</sup>† Anju Panthi,<sup>1</sup>★ Manan Agarwal<sup>1</sup>,<sup>1</sup> Sindhu Pandey<sup>1</sup>,<sup>2</sup>★ Khushboo K. Rao<sup>1</sup>,<sup>1</sup> Vikrant Jadhav<sup>1</sup>,<sup>3,4</sup> and Annapurni Subramaniam<sup>3</sup>

<sup>1</sup>Department of Physics, Birla Institute of Technology and Science – Pilani, Pilani 333031, Rajasthan, India

<sup>2</sup>Aryabhata Research Institute of Observational Sciences, Manora Peak, Nainital 263001, India

<sup>3</sup>Indian Institute of Astrophysics, Sarjapur Road, Koramangala, Bangalore 560034, India

<sup>4</sup>Joint Astronomy Programme and Department of Physics, Indian Institute of Science, Bangalore 560012, India

Accepted 2022 January 18. Received 2022 January 17; in original form 2021 November 23

## UOCS – XI. Study of blue straggler stars in open cluster NGC 7142 using UVIT/AstroSat

Anju Panthi,<sup>1</sup>★ Kaushar Vaidya<sup>1</sup>,<sup>1</sup>★ Nagaraj Vernekar<sup>1</sup>,<sup>2</sup>★ Annapurni Subramaniam,<sup>3</sup> Vikrant Jadhav<sup>1</sup>,<sup>4</sup> and Manan Agarwal<sup>1</sup>,<sup>5</sup>

<sup>1</sup>Department of Physics, Birla Institute of Technology and Science, Pilani, Rajasthan 333031, India

<sup>2</sup>Dipartimento di Fisica e Astronomia "Galileo Galilei", Università di Padova, Vicolo dell'Osservatorio 3, I-35122, Padova, Italy

<sup>3</sup>Indian Institute of Astrophysics, Sarjapur Road, Koramangala, Bangalore 560034, India

<sup>4</sup>Helmholtz-Institut für Strahlen- und Kernphysik, Universität Bonn, Nussallee 14-16, D-53115 Bonn, Germany

<sup>5</sup>Anton Pannekoek Institute for Astronomy & GRAPPA, University of Amsterdam, Science Park 904, NL-1098 XH Amsterdam, the Netherlands

Accepted 2023 November 28. Received 2023 November 24; in original form 2023 August 1

THE ASTRONOMICAL JOURNAL, 168:97 (11pp), 2024 September

© 2024. The Author(s). Published by the American Astronomical Society.

**OPEN ACCESS**

## UOCS XIV: Study of the Open Cluster NGC 2627 Using UVIT/AstroSat

Pinapati Saketh, Anju Panthi<sup>1</sup>, and Kaushar Vaidya

Department of Physics, Birla Institute of Technology and Science, Pilani, Rajasthan-333031, India; [f20200966@pilani.bits-pilani.ac.in](mailto:f20200966@pilani.bits-pilani.ac.in),

[p20190413@pilani.bits-pilani.ac.in](mailto:p20190413@pilani.bits-pilani.ac.in), [kaushar@pilani.bits-pilani.ac.in](mailto:kaushar@pilani.bits-pilani.ac.in)

Received 2024 April 13; revised 2024 June 16; accepted 2024 June 17; published 2024 July 31

<https://doi.org/10.3847/1538-388>

## UOCS –VIII. UV study of the open cluster NGC 2506 using ASTROSAT★

Anju Panthi,<sup>1</sup>† Kaushar Vaidya<sup>1</sup>,<sup>1</sup>† Vikrant Jadhav<sup>1</sup>,<sup>2,3,4</sup>† Khushboo K. Rao<sup>1</sup>,<sup>1</sup> Annapurni Subramaniam,<sup>2</sup> Manan Agarwal<sup>1</sup>,<sup>5</sup> and Sindhu Pandey<sup>1</sup>,<sup>6</sup>

<sup>1</sup>Department of Physics, Birla Institute of Technology and Science, Pilani 333031, India

<sup>2</sup>Indian Institute of Astrophysics, Sarjapur Road, Koramangala, Bangalore 560034, India

<sup>3</sup>Joint Astronomy Programme and Department of Physics, Indian Institute of Science, Bangalore 560012, India

<sup>4</sup>Inter-University Centre for Astronomy and Astrophysics, Post Bag 4, Ganeshkhind, Pune, Maharashtra 411007, India

<sup>5</sup>Department of Physics and Kavli Institute for Astrophysics and Space Research, Massachusetts Institute of Technology, Cambridge, MA 02139, USA

<sup>6</sup>Aryabhata Research Institute of Observational Sciences, Manora Peak, Nainital 263001, India

Accepted 2022 August 23. Received 2022 August 23; in original form 2022 May 16

## UOCS-XII. A study of open cluster NGC 6940 using UVIT/AstroSat cluster properties and exotic populations

Anju Panthi★ and Kaushar Vaidya<sup>1</sup>,<sup>1</sup>★

Department of Physics, Birla Institute of Technology and Science, Pilani 333031, Rajasthan, India

Accepted 2023 December 14. Received 2023 December 12; in original form 2023 September 22

## Field blue straggler stars: discovery of white dwarf companions to blue metal-poor stars using UVIT/AstroSat

Anju Panthi,<sup>1</sup>★ Annapurni Subramaniam,<sup>2</sup>★ Kaushar Vaidya<sup>1</sup>,<sup>1</sup>★ Vikrant Jadhav<sup>1</sup>,<sup>3</sup> Sharmila Rani,<sup>2</sup> Sivarani Thirupathi<sup>2</sup> and Sindhu Pandey<sup>1</sup>,<sup>4</sup>

<sup>1</sup>Department of Physics, Birla Institute of Technology and Science, Pilani, Rajasthan-333031, India

<sup>2</sup>Indian Institute of Astrophysics, Sarjapur Road, Koramangala, Bangalore 560034, India

<sup>3</sup>Helmholtz-Institut für Strahlen- und Kernphysik, Universität Bonn, Nussallee 14-16, D-53115 Bonn, Germany

<sup>4</sup>Aryabhata Research Institute of Observational Sciences, Manora Peak, Nainital 236002, India

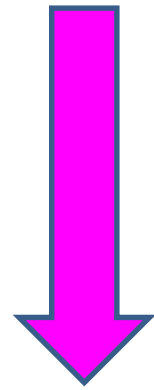
Accepted 2023 July 31. Received 2023 July 27; in original form 2023 May 15

## What are blue straggler stars (BSS)?

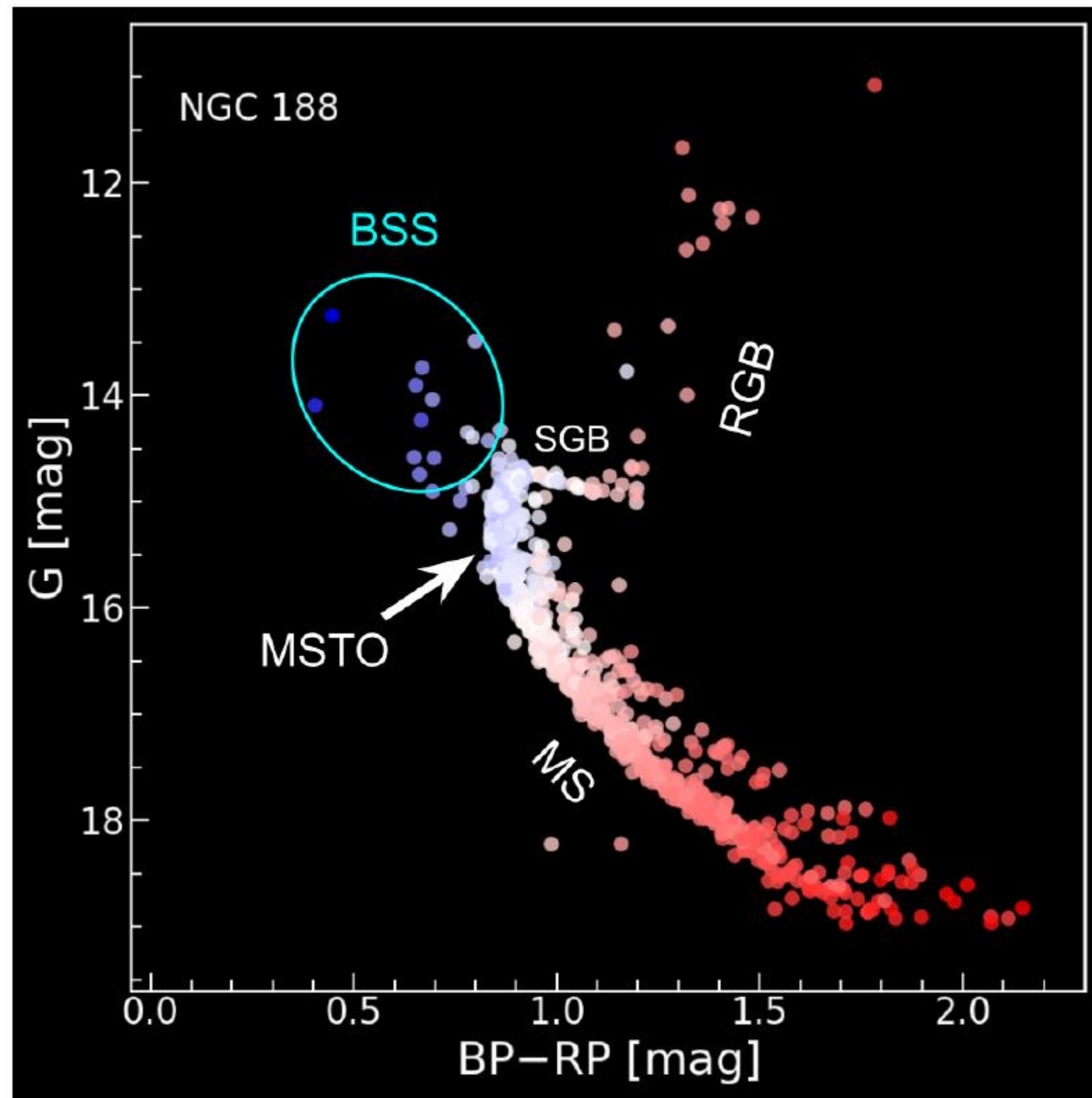
Stars that are “Brighter and Bluer” compared to the main-sequence turnoff (MSTO) of a star cluster

## What are blue straggler stars (BSS)?

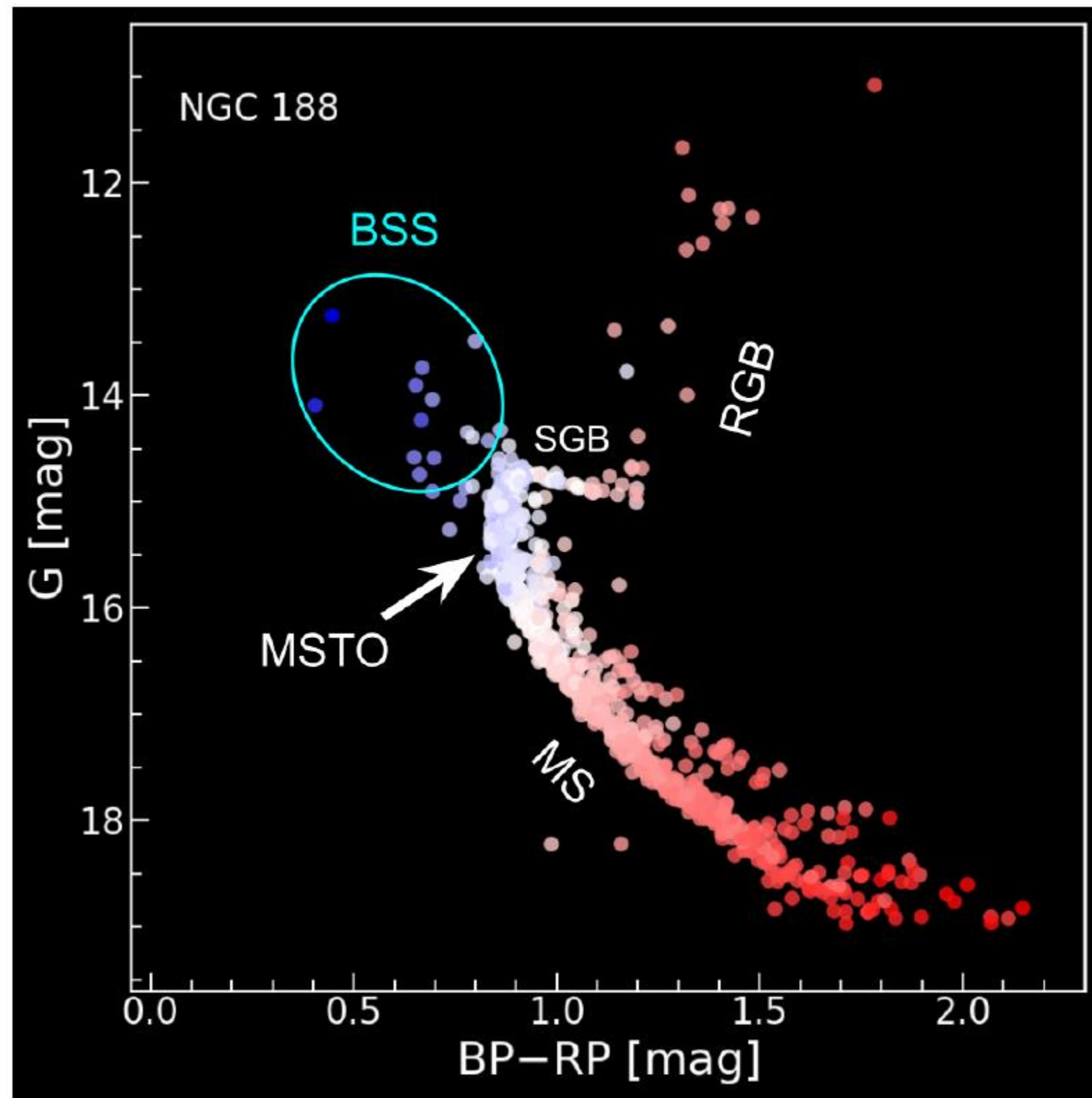
Stars that are “Brighter and Bluer” compared to the main-sequence turnoff (MSTO) of a star cluster



Extended main-sequence lifetimes



A color-magnitude diagram of NGC 188 from Rao et al. (2023) showing cluster members (membership probabilities  $> 0.6$ ).

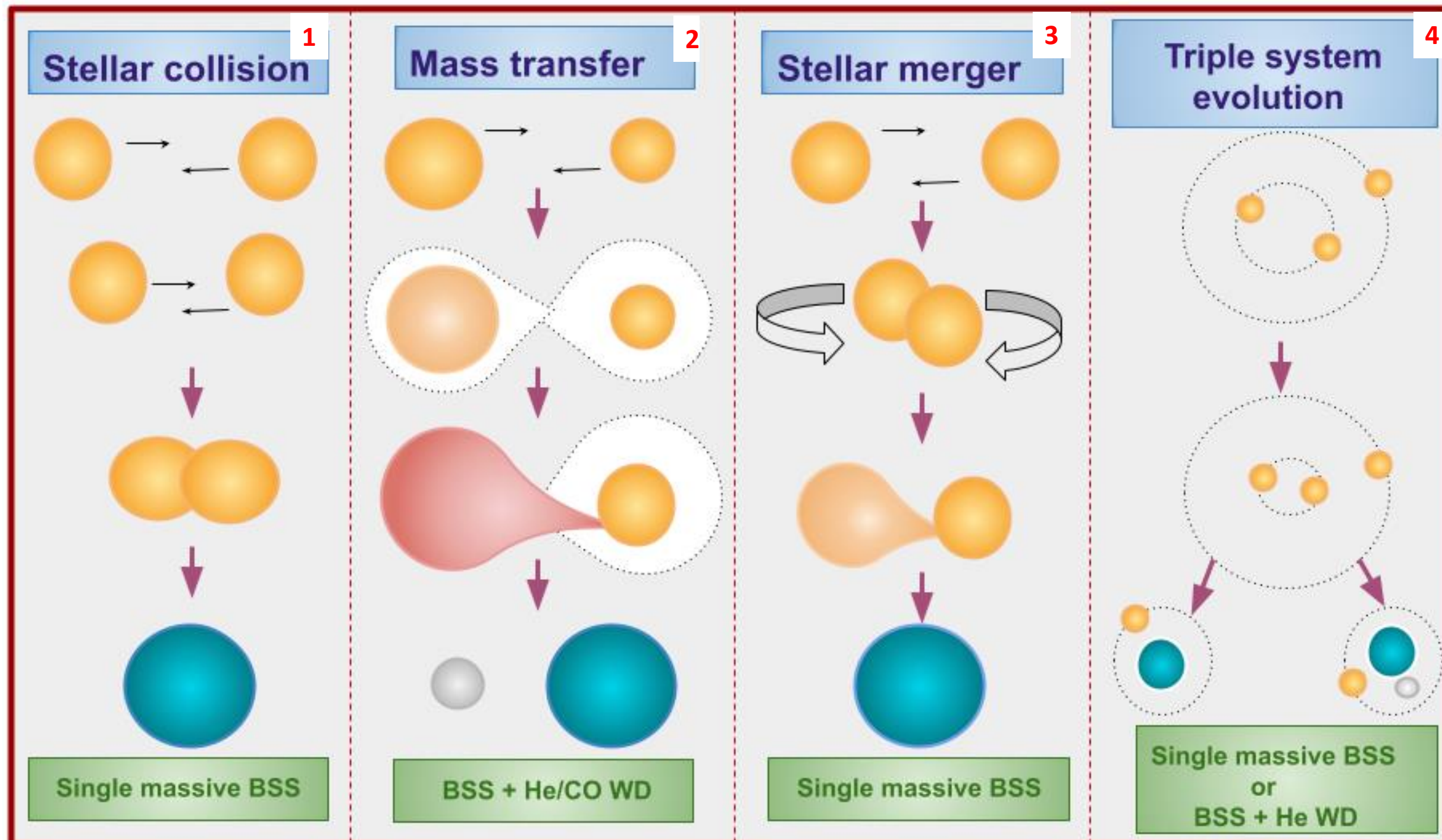


**Why do BSS lag in their evolution?**

A color-magnitude diagram of NGC 188 from Rao et al. (2023) showing cluster members (membership probabilities > 0.6).



# Formation Mechanisms



↑  
Not viable in open clusters and fields

**1** Hills & Day 1976, Hurley et al. 2005, Chatterjee et al. 2013, Leonard 1989

**2** McCrea 1964, Webbink 1976, Chen & Han 2008

**3** McCrea 1964, Perets et al. 2009

**4** Kozai 1962, Perets et al. 2009

## Where are BSS found?

- ❖ Globular clusters (Sandage 1953)
- ❖ Open clusters (Leiner et al. 2021, Jadhav and Subramaniam 2021)
- ❖ Galactic fields (Preston et al. 1994)
- ❖ Dwarf galaxies (Momany et al. 2007)
- ❖ Numbers of BSS range from **10 to 400** in globular clusters (Bailyn 1995, Davies et al. 2004)
- ❖ Numbers of BSS range from **1 to ~35** in open clusters (Jadhav and Subramaniam 2021)

## Field Blue Metal-Poor (BMP) Stars

- ❖ Preston and Snedon (2000) and Carney et al. (2001) found **high-velocity, blue metal-poor stars** having main-sequence gravities

## Field Blue Metal-Poor (BMP) Stars

- ❖ Preston and Snedon (2000) and Carney et al. (2001) found **high-velocity, blue metal-poor stars** having main-sequence gravities

**Intermediate-age Dwarf  
galaxy stars accreted by  
Milky-Way Galaxy**



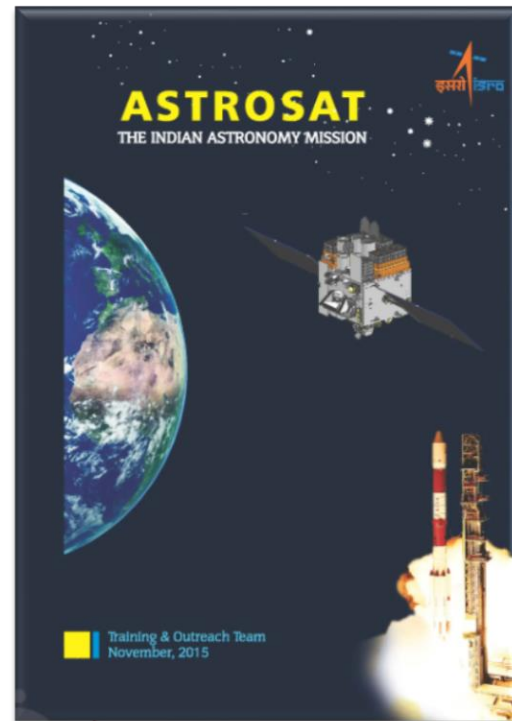
**Field Blue Stragglers**

## Field Blue Metal-Poor (BMP) Stars

- ❖  $2/3^{\text{rd}}$  of BMP are **single-lined spectroscopic binaries** (Preston et al. 2000)
- ❖ A fraction also shows enhancement in C, Sr, and Ba

# Motivation

- ❖ Investigate the formation mechanisms of BSS (Geller & Mathieu 2011; Gosnell et al. 2014; Subramaniam et al. 2016)
- ❖ Know the relative importance of different formation mechanisms in diverse environments

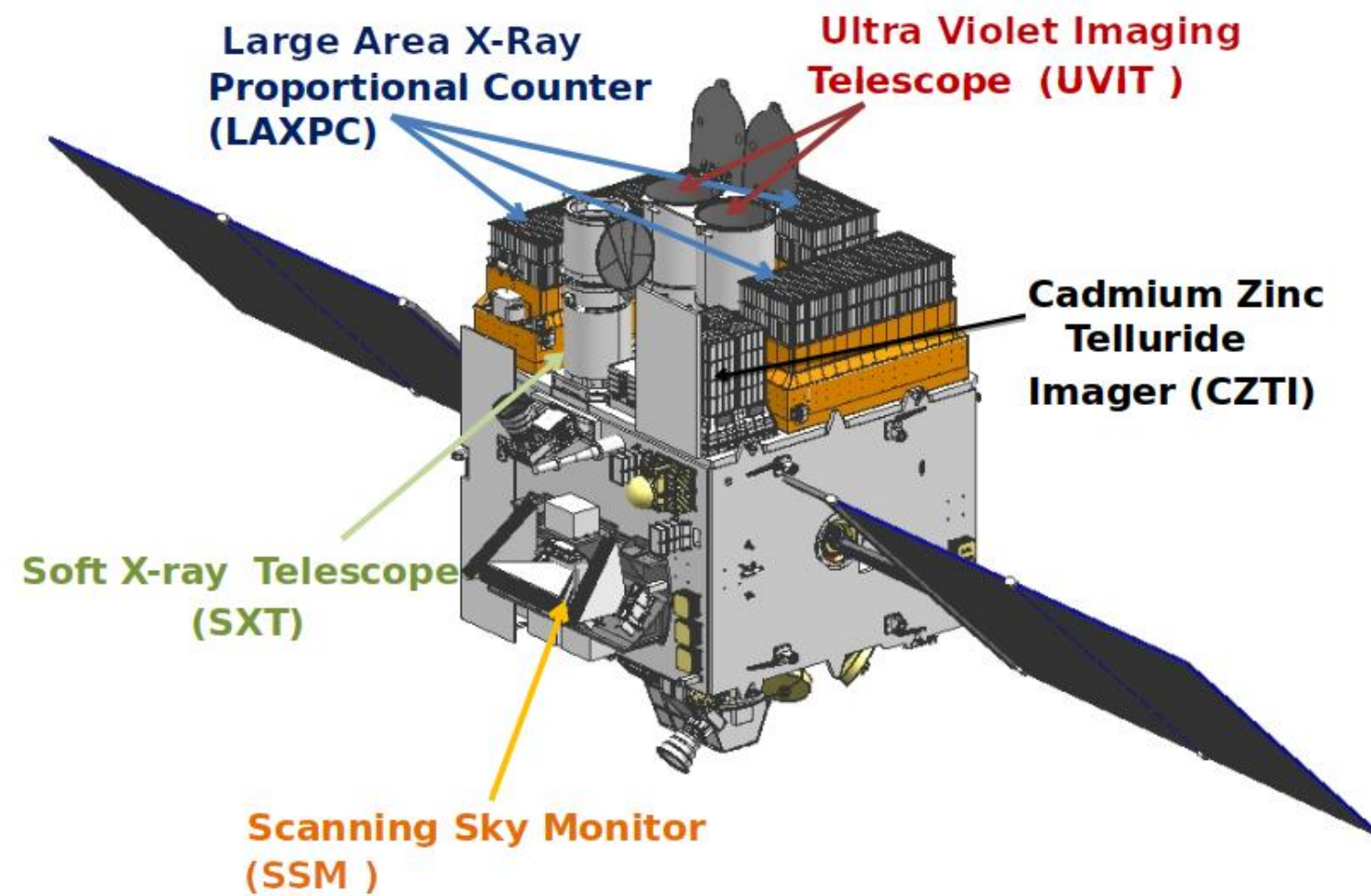


UV imaging observations to identify BSS and search for hot companions



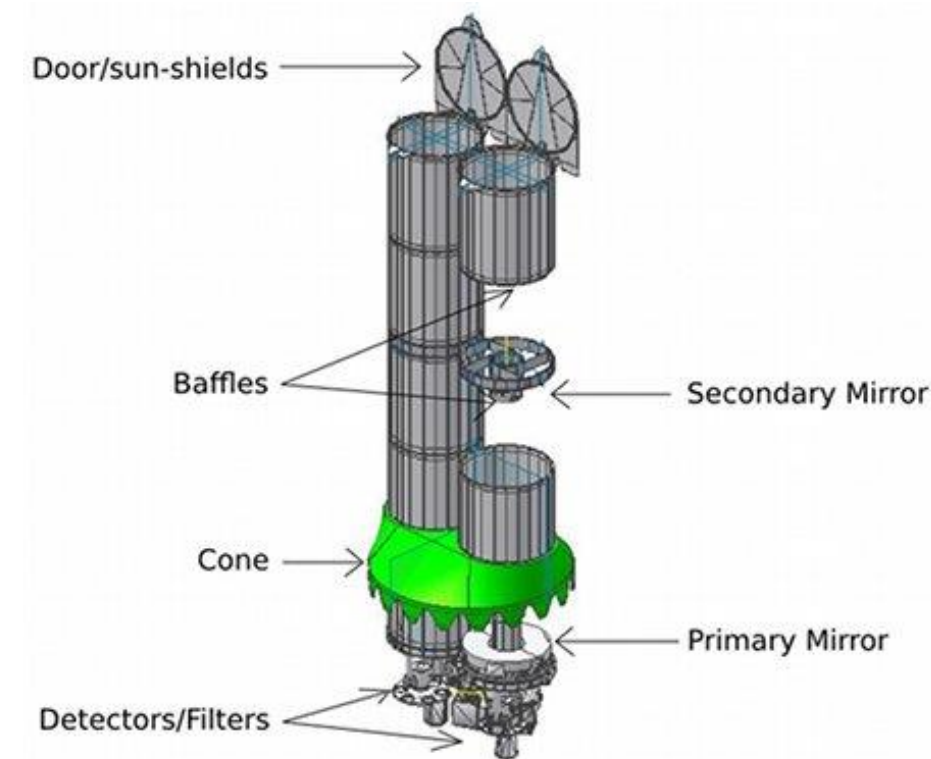
Search for variable signature and obtain the parameters of binary components

# Ultraviolet Imaging Telescope (UVIT)



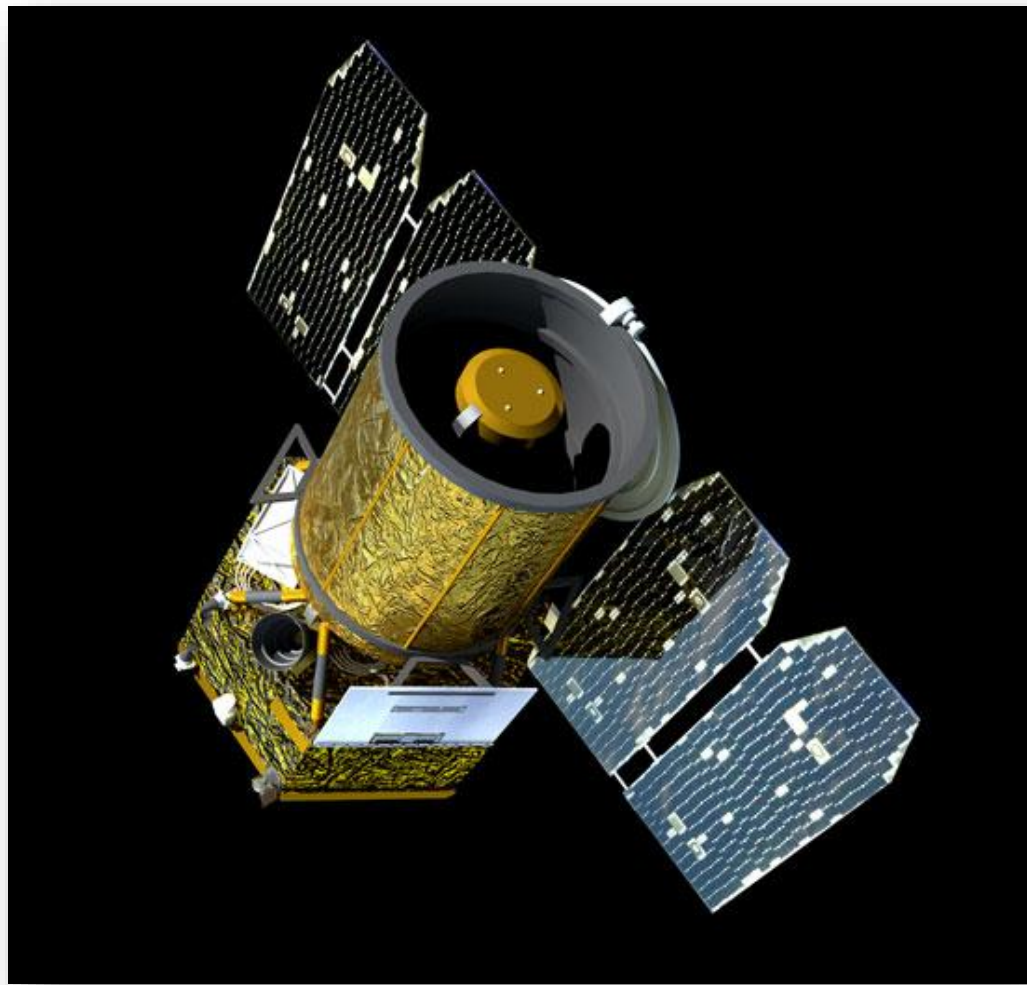
Agrawal, P. C. et al. (2016)

- ❖ Two 38 cm telescopes: FUV (130 nm -180 nm), NUV (200-300 nm) & VIS (350-550 nm)
- ❖ Spatial resolution of 1.2" (NUV filter) & ~ 1.5" (FUV filter) (GALEX ~ 5")
- ❖ Field of view of 0.5 degree (GALEX ~ 1.2 degrees)

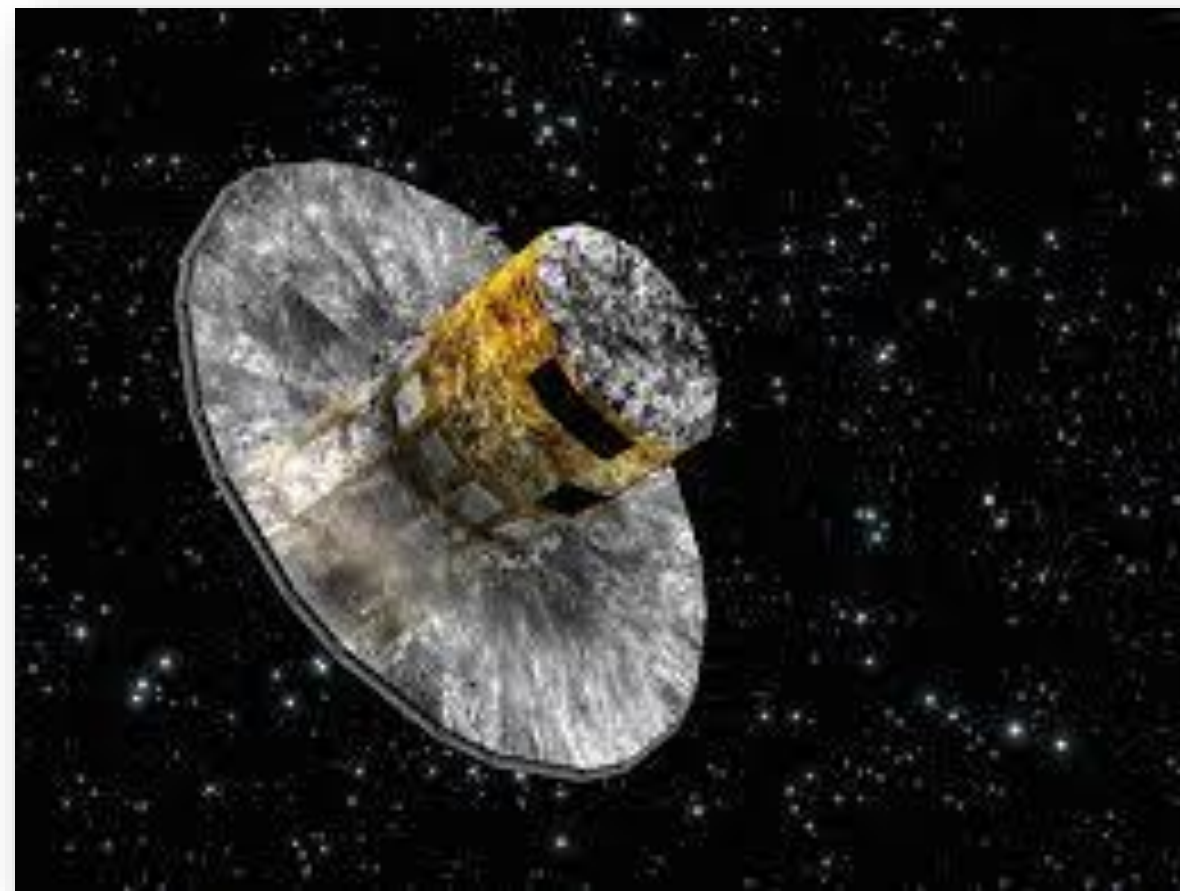


Tandon et al. (2017)





**GALEX (1350 Å - 2800 Å)**



**GAIA (5109 Å - 8578 Å)**



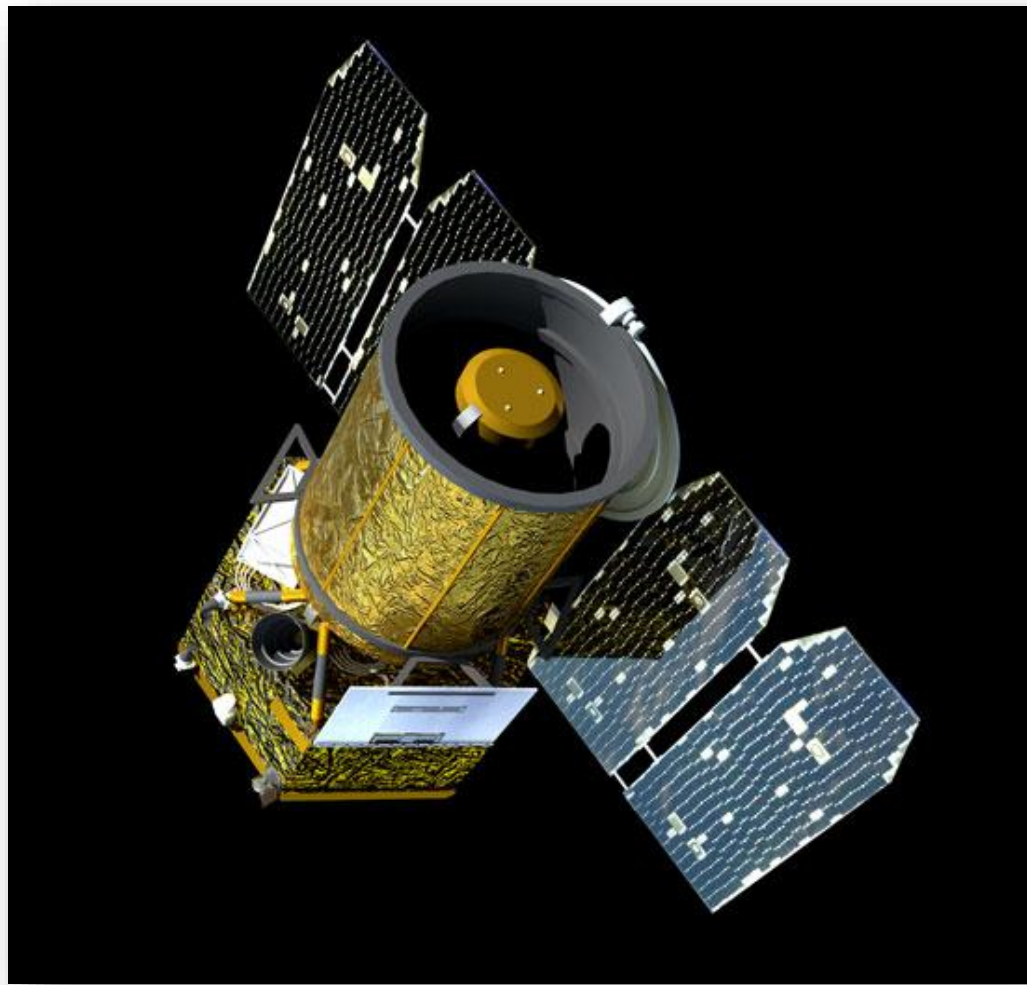
**PANSTARRS (3900 Å - 5400 Å)**



**2MASS (12350 Å - 21590 Å)**



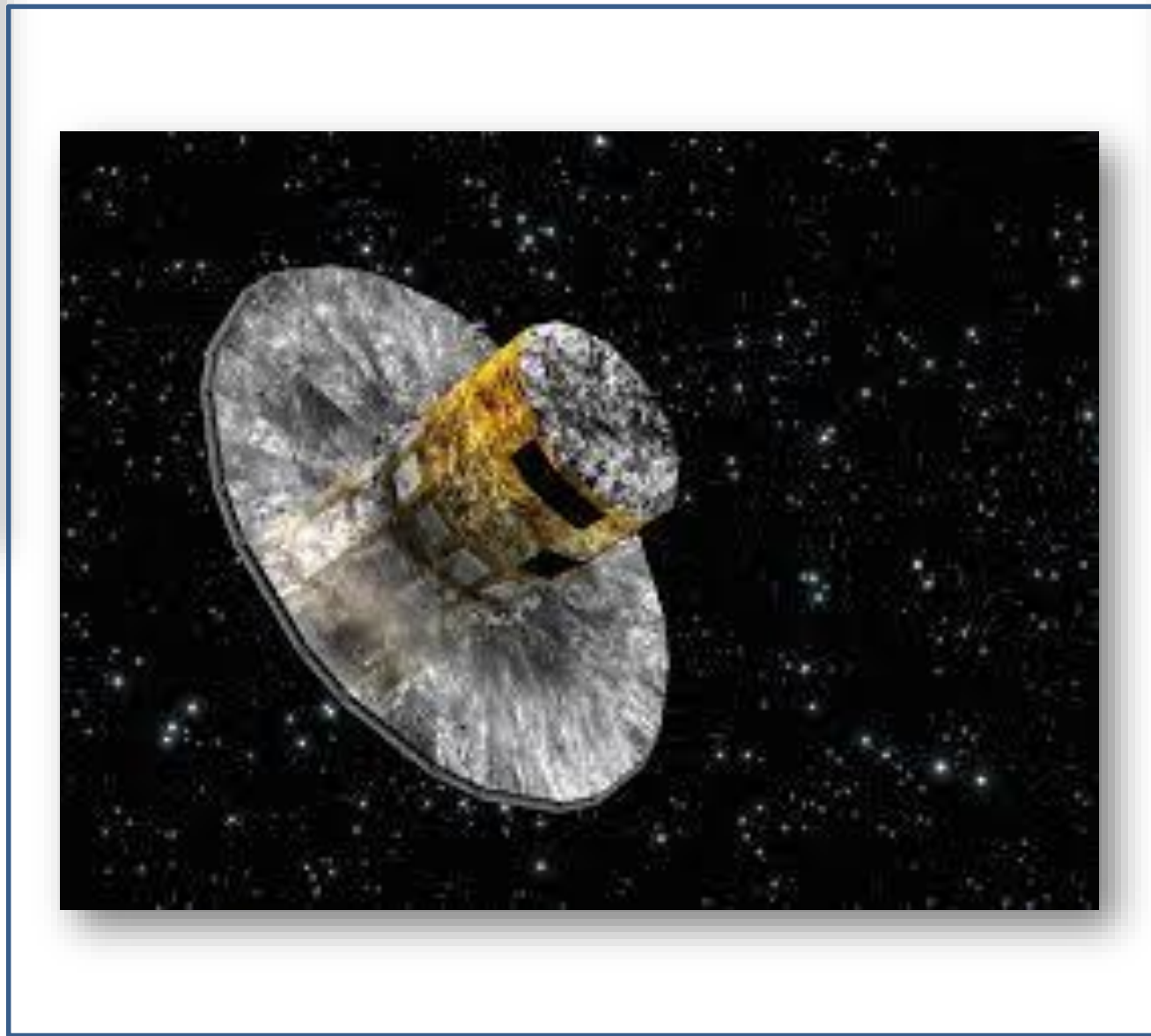
**WISE (33526 Å - 280883 Å)**



**GALEX (1350 Å - 2800 Å)**

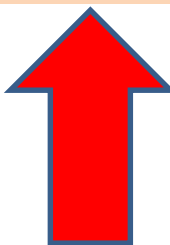


**2MASS (12350 Å - 21590 Å)**



**GAIA (5109 Å - 8578 Å)**

**Cluster Membership**



**PANSTARRS (3900 Å - 5400 Å)**



**WISE (33526 Å - 280883 Å)**

## Target Clusters

Name	Age (Gyr)	[Fe/H]	Distance (pc)	E(B-V)
NGC 7789	1.6	-0.02	2075	0.28
NGC 2506	2	-0.52	3110	0.08
NGC 7142	4	0	2000	0.1
NGC 6940	1	-0.09	770	0.4
NGC 2627	1.9	-0.10	1837	0.1

## Cluster Membership

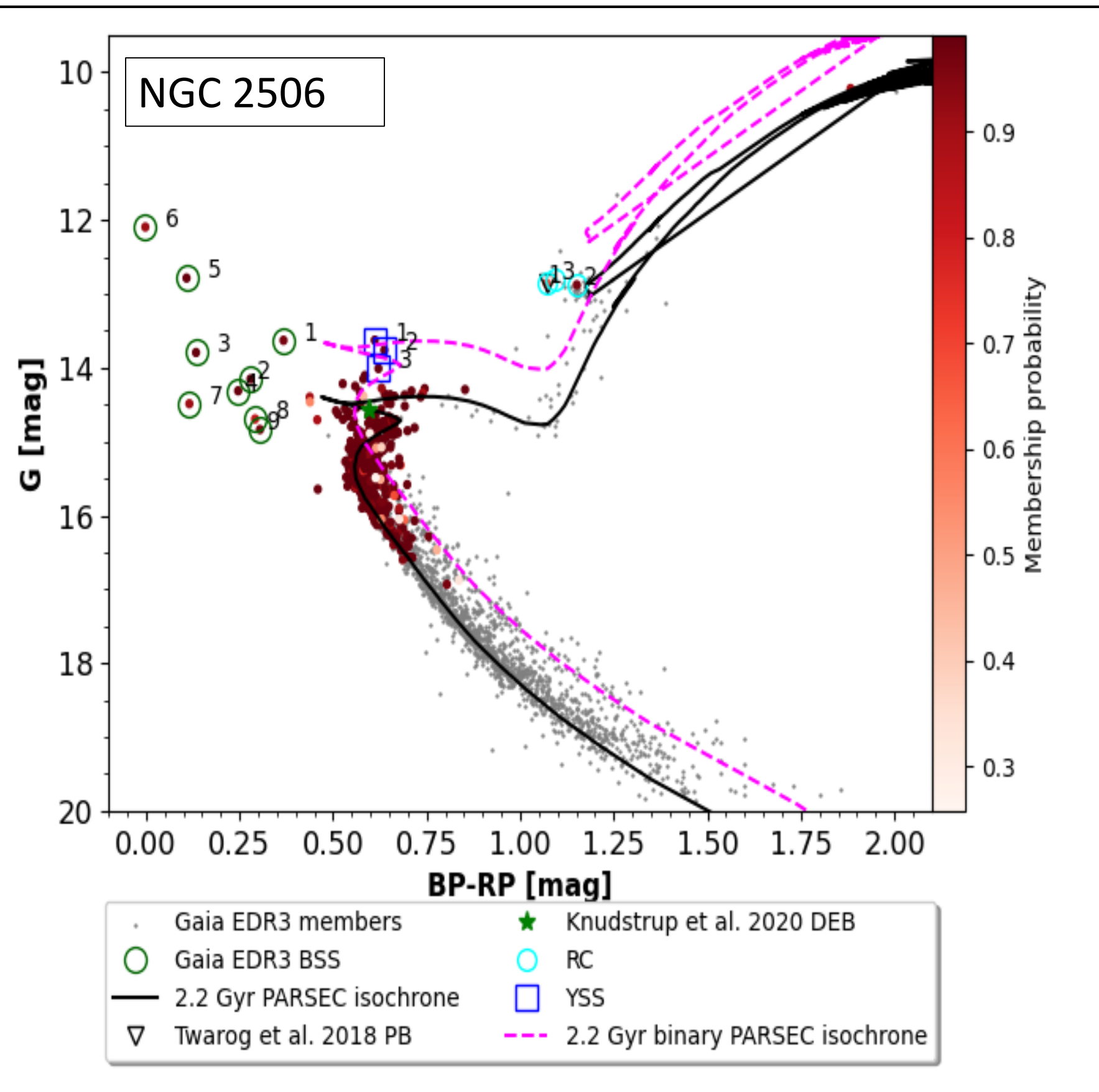
- ❖ **ML-MOC** (Agarwal et al. 2021) on Gaia DR3 data
- ❖ Identification of cluster members down to  $G = 20$  mag
- ❖ Estimated contamination: 2 – 12% (Agarwal et al. 2021)
- ❖ Estimated completeness: 90% till  $G = 19$  mag (Bhattacharya et al. 2022)

# UV Photometry

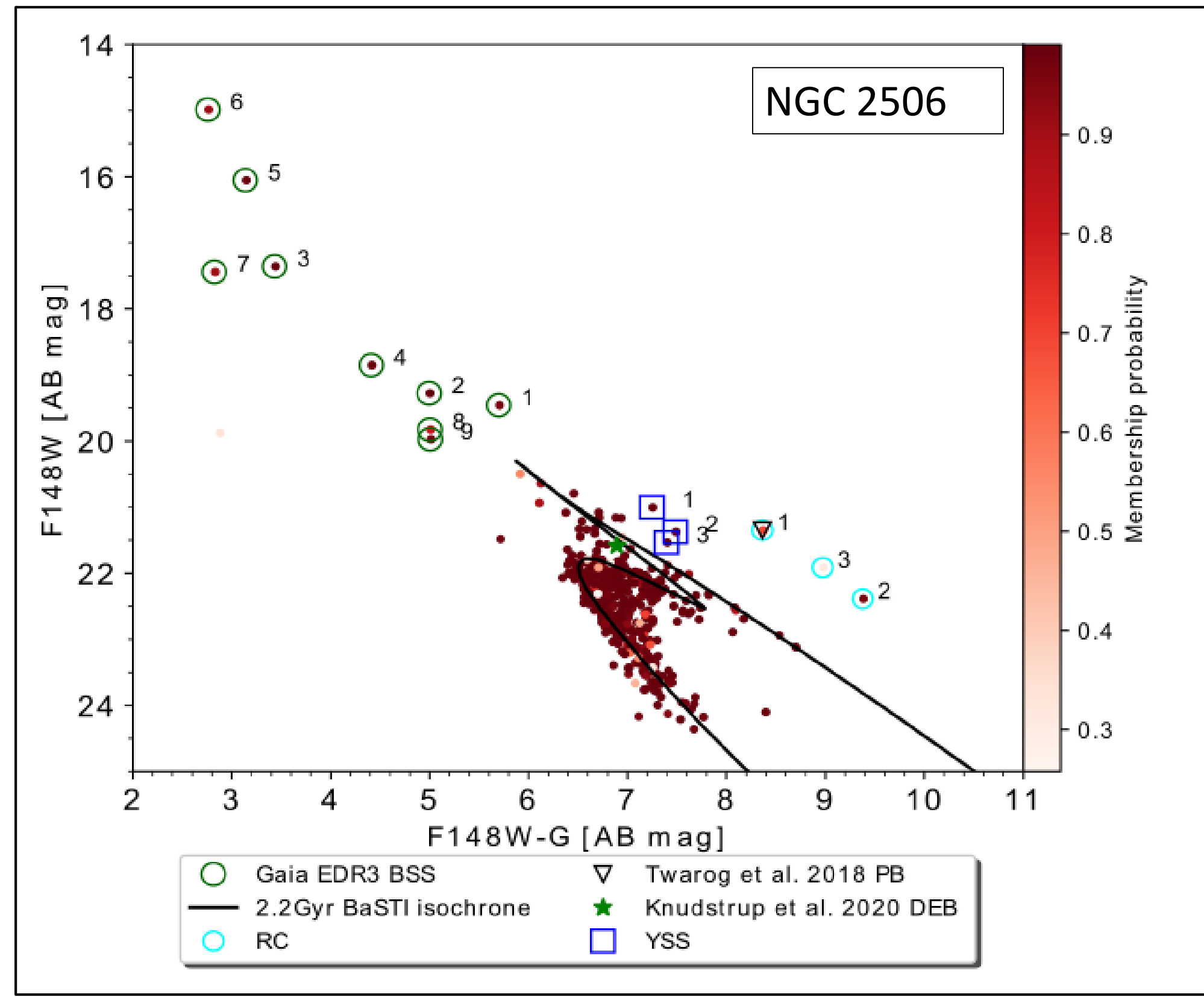
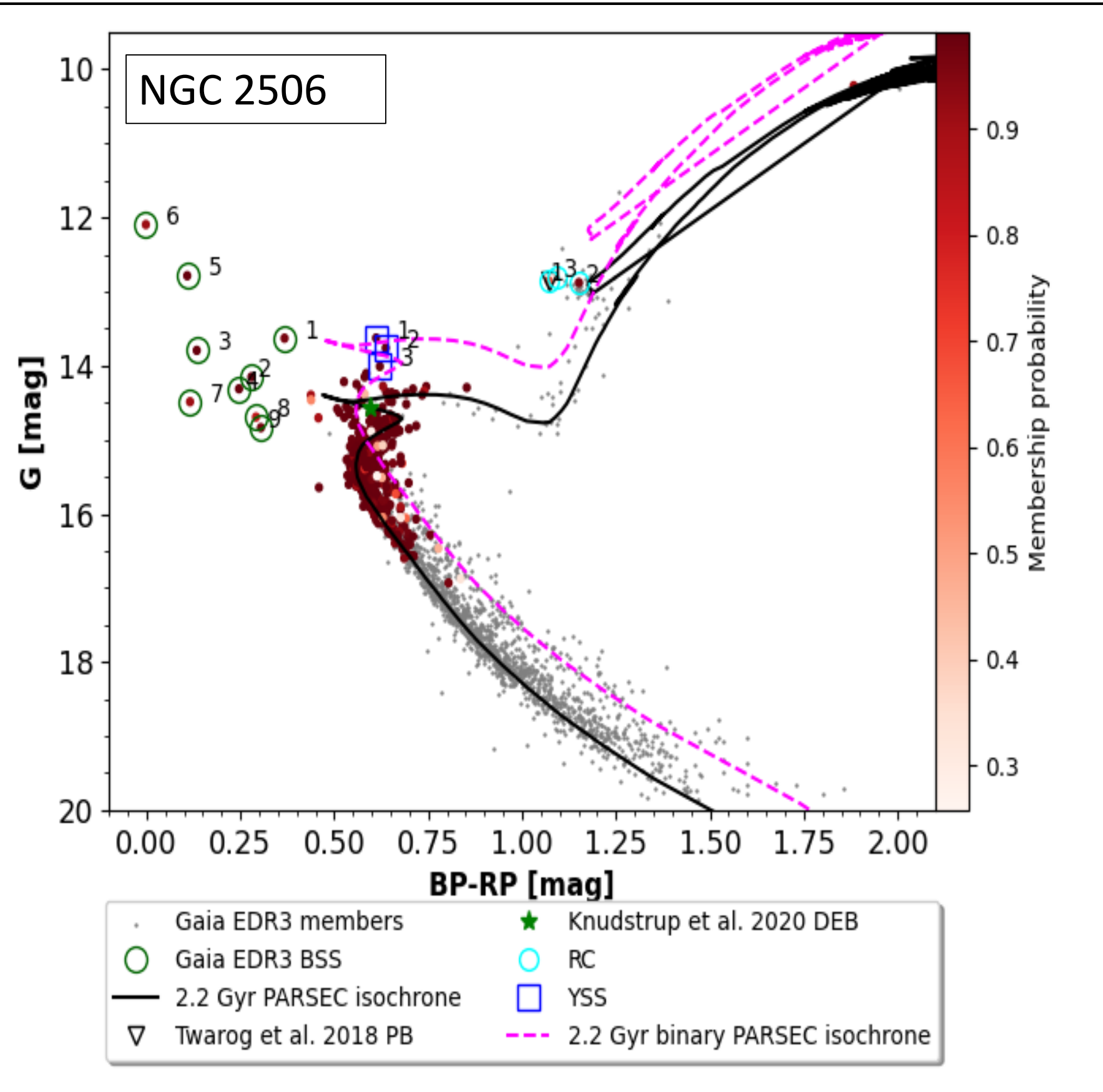
- ❖ **CCDLAB** ([Postma et al. 2017](#)) to convert Level-1 data into science-ready images
- ❖ Photometry using IRAF ([Barnes 1993](#))
- ❖ Aperture correction, PSF correction, and Saturation correction to obtain final magnitudes in NUV and FUV in AB magnitude system

## Details of UVIT Observations

Cluster	Observation Date	Filters	Exposure (sec)
NGC7789	July 2017	FUV: F169M NUV: N245M N263M N279N	609 3219 1142 1021
NGC2506	October 2019	FUV: F148W F154W F169M	9224 7499 7027
NGC7142	June 2018	FUV: F148W	2280
NGC6940	June 2018	FUV: F169M	2000
NGC2627	June 2020	FUV: F148W F169M	1370 4062
<b>Fields</b>	<b>Sep 2021</b>	<b>FUV: F148W F169M</b>	<b>200-2000</b>



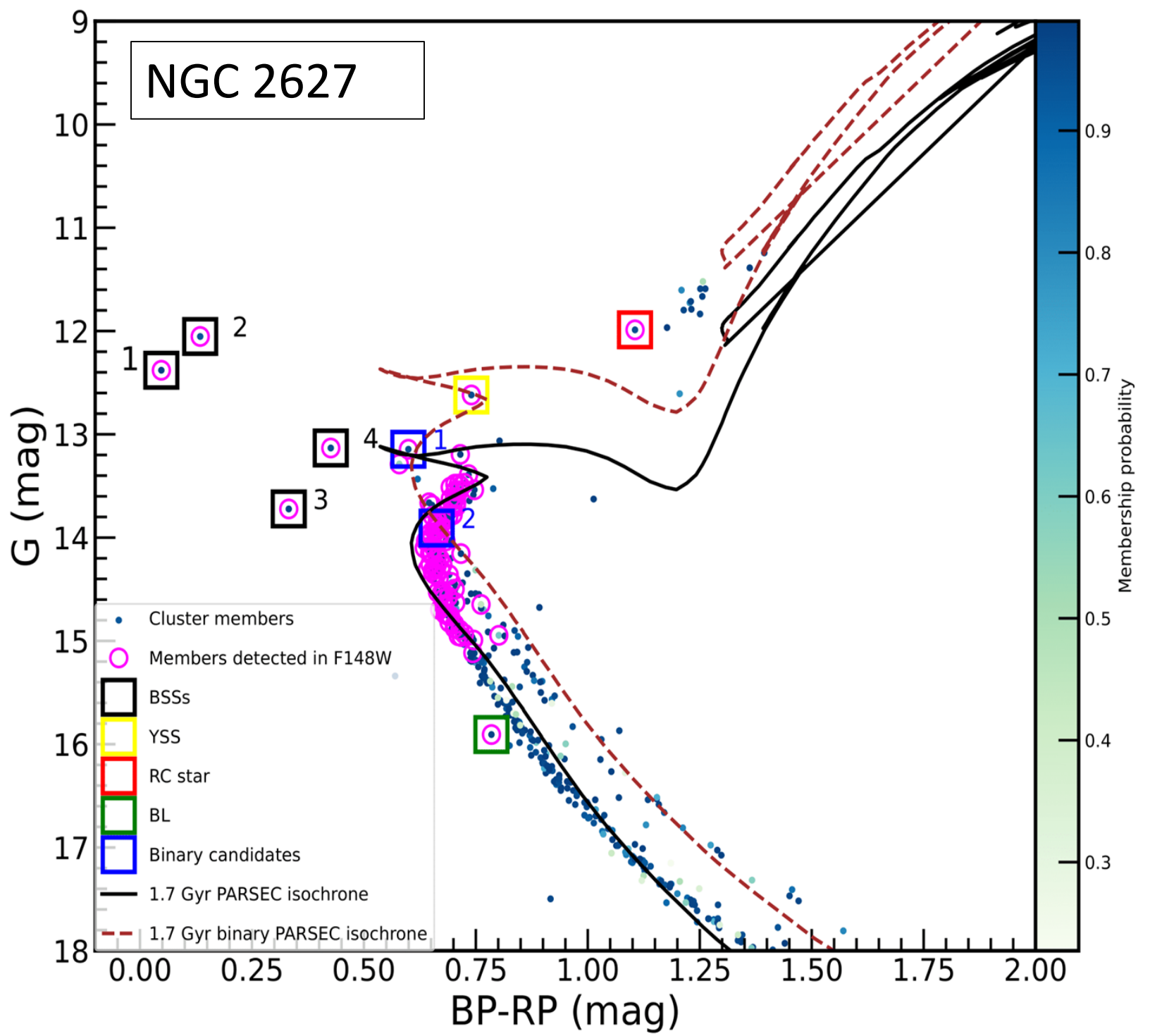
Distance: 3110 pc;  $E(\text{BP-RP}) = 0.155$ ;  $A_G : 0.39$



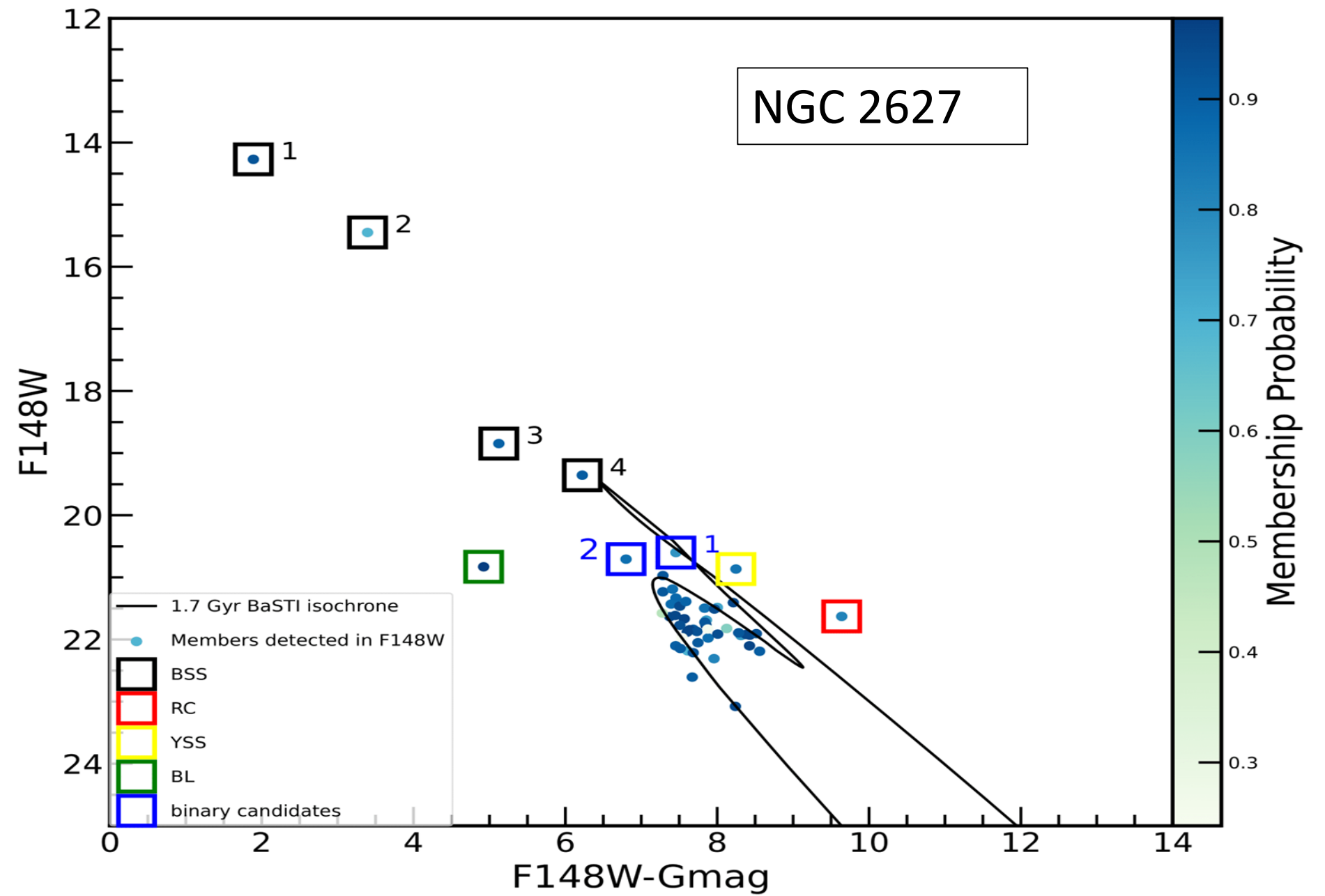
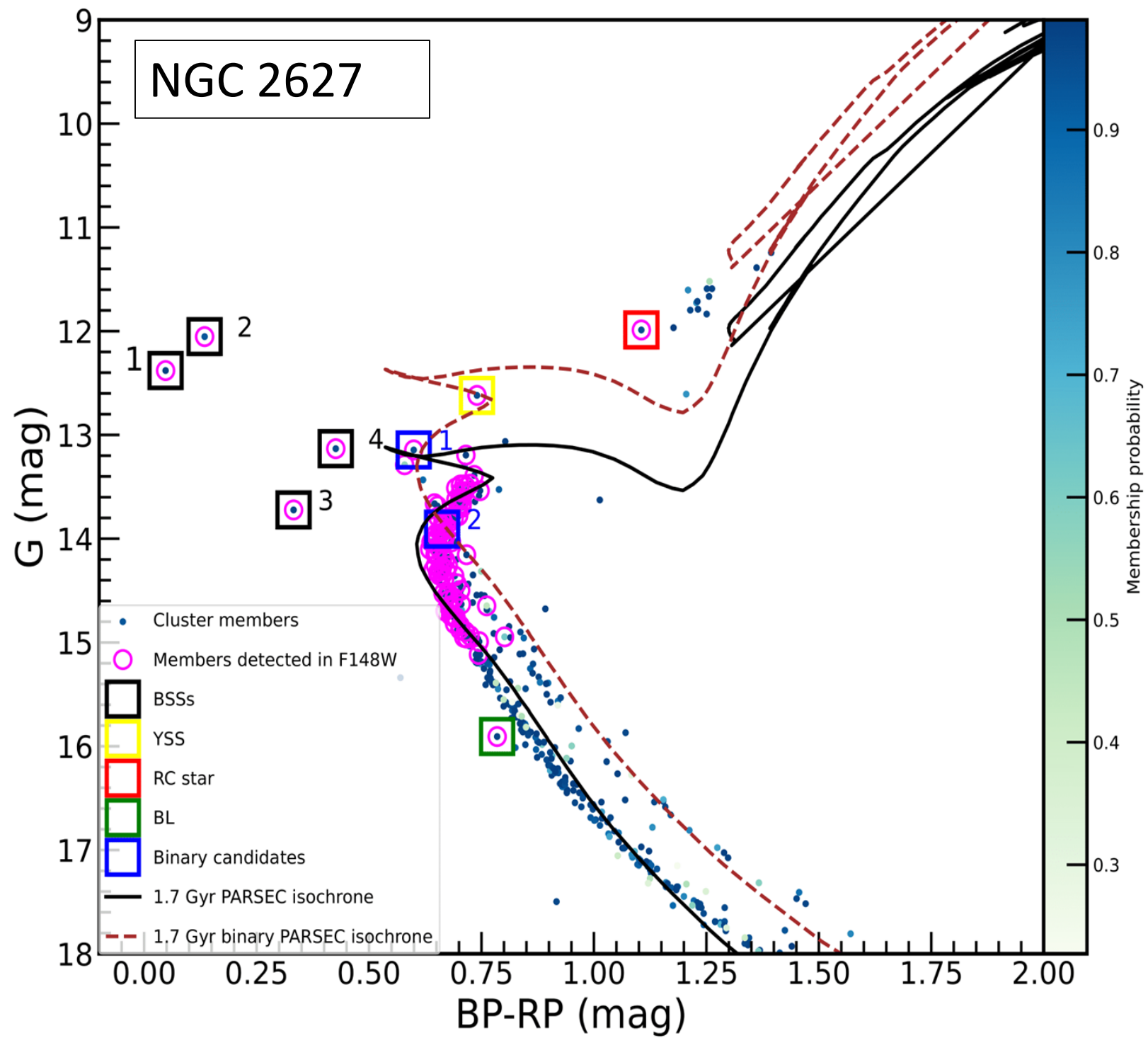
$E(F148W-G) = 0.473; A_{F148W} : 0.721$

Distance: 3110 pc;  $E(BP-RP) = 0.155; A_G : 0.39$





Distance: 1837 pc;  $E(\text{BP-RP}) = 0.155$ ;  $A_G : 0.39$

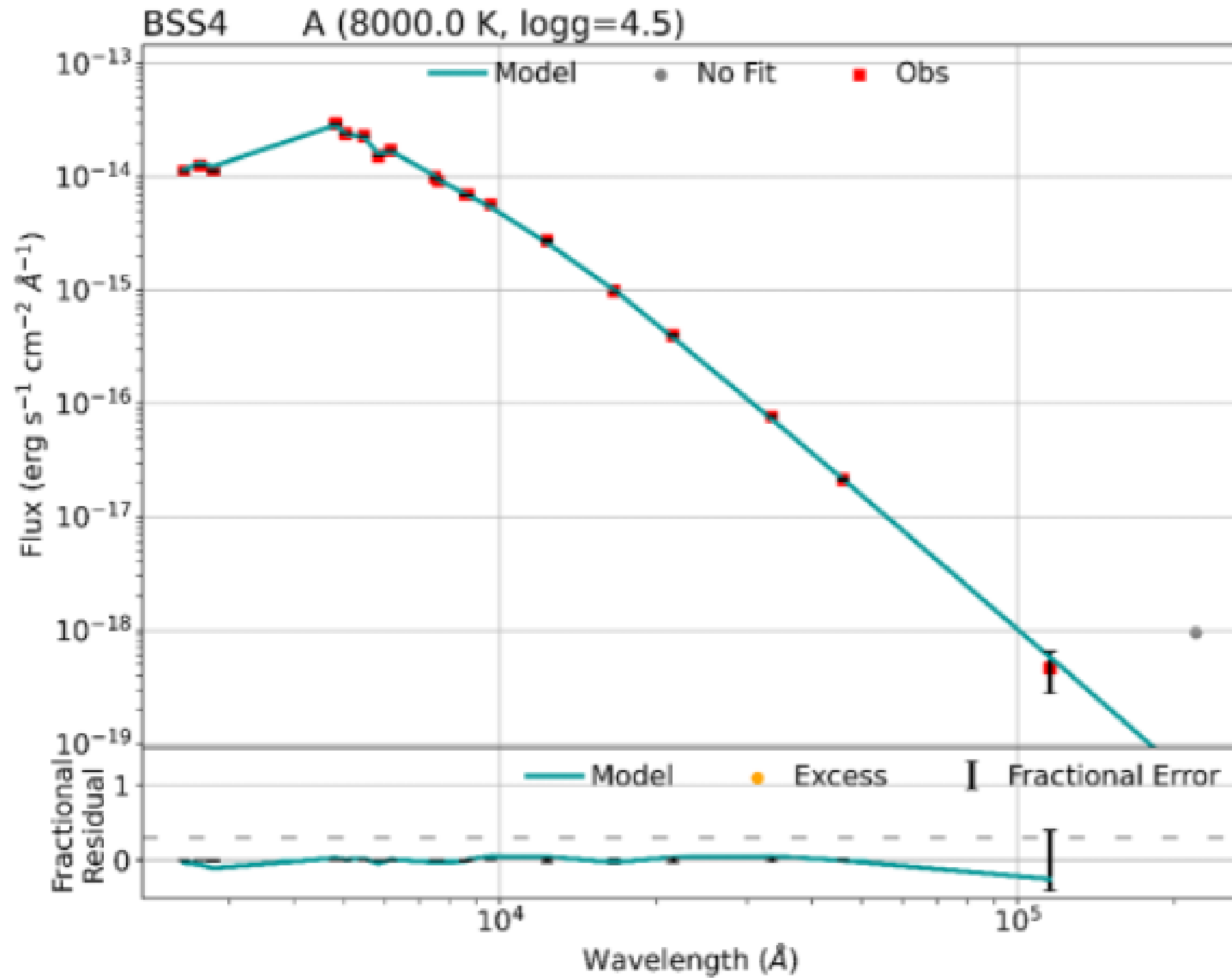


$$E(F148W-G) = 0.35; A_{F148W} : 0.741$$

Distance: 1837 pc;  $E(Bp-Rp) = 0.12$ ;  $A_G : 0.372$

# Construction of Spectral Energy Distributions

- ❖ SEDs constructed using **Virtual Observatory of SED Analyzers (VOSA)**
  - ❖ Compilation of photometry
  - ❖ Correction of extinction (**Fitzpatrick 1999, Indebetouw 2005**)
  - ❖ Calculation of synthetic photometry based on model (**Single: Kurucz stellar models by Castelli et al. 1997; Binary: Koester et al. 2010**)
- ❖ SED fitting by minimization of  $\chi^2$
- ❖ Multi-wavelength photometry from UV to Mid-IR



# BSS SEDs showing UV-excess in Clusters and Fields

Cluster name	Single-component SEDs	Excess in UV fluxes
<b>NGC 7789</b>	8 BSS	7 BSS
<b>NGC 2506</b>	4 BSS	3 BSS
<b>NGC 7142</b>	0	7 BSS
<b>NGC 6940</b>	1 BSS	0
<b>NGC 2627</b>	2 BSS	2 BSS
<b>Galactic Fields</b>	10 BMP	17 BMP

# BSS SEDs showing UV-excess in Clusters and Fields

Cluster name	Single-component SEDs	Excess in UV fluxes
<b>NGC 7789</b>	8 BSS	7 BSS
<b>NGC 2506</b>	4 BSS	3 BSS
<b>NGC 7142</b>	0	7 BSS
<b>NGC 6940</b>	1 BSS	0
<b>NGC 2627</b>	2 BSS	2 BSS
<b>Galactic Fields</b>	10 BMP	17 BMP

Chromospheric Activity (Hall 2008)

Hot Spots (Kouzuma 2019)

Coronal Activity (Stelzer et al. 2016)

A hot companion

?

# BSS SEDs showing UV-excess in Clusters and Fields

Cluster name	Single-component SEDs	Excess in UV fluxes
<b>NGC 7789</b>	8 BSS	7 BSS
<b>NGC 2506</b>	4 BSS	3 BSS
<b>NGC 7142</b>	0	7 BSS
<b>NGC 6940</b>	1 BSS	0
<b>NGC 2627</b>	2 BSS	2 BSS
<b>Galactic Fields</b>	10 BMP	17 BMP

Chromospheric Activity (Hall 2008)

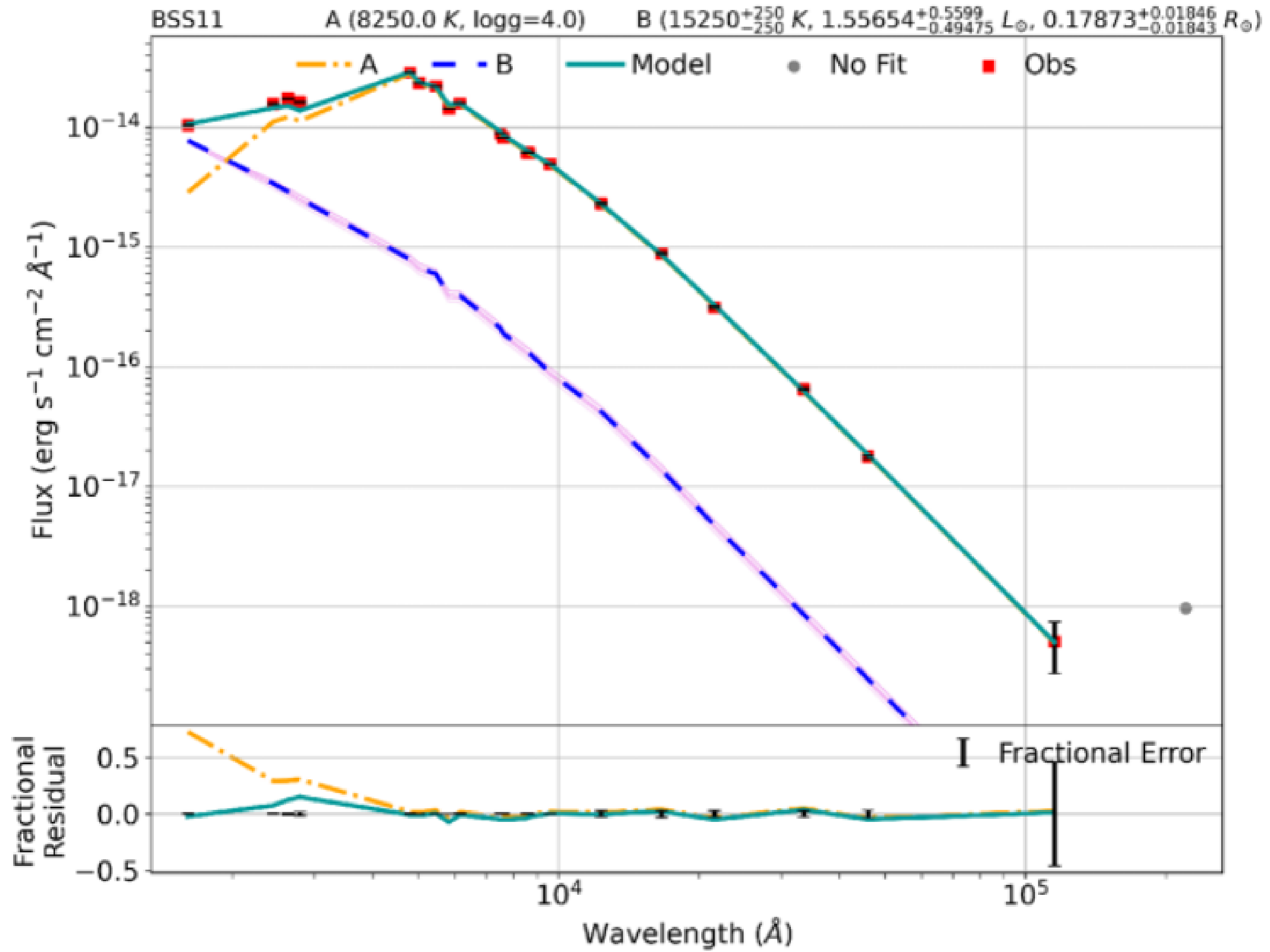
Hot Spots (Kouzuma 2019)

Coronal Activity (Stelzer et al. 2016)

A hot companion



14/19 BSS not detected in XMM/Chandra. The remaining not observed by XMM/Chandra





## BSS Properties

---

Target	Objects	Temperature (K)	Luminosity ( $L_{\odot}$ )	Radius ( $R_{\odot}$ )
NGC 7789	BSSs	7250 – 10250	7.43 – 122.8	1.62 – 4.08
NGC 2506	BSSs	7750 – 9750	10.58 – 84.37	1.51 – 3.38
NGC 7142	BSSs	6500 – 7500	8.72 – 26.97	2.04 – 4.09
NGC 6940	BSSs	8500	32.58	2.63
NGC 2627	BSSs	8000 – 10750	10.55 – 60.03	1.69 – 2.86

---

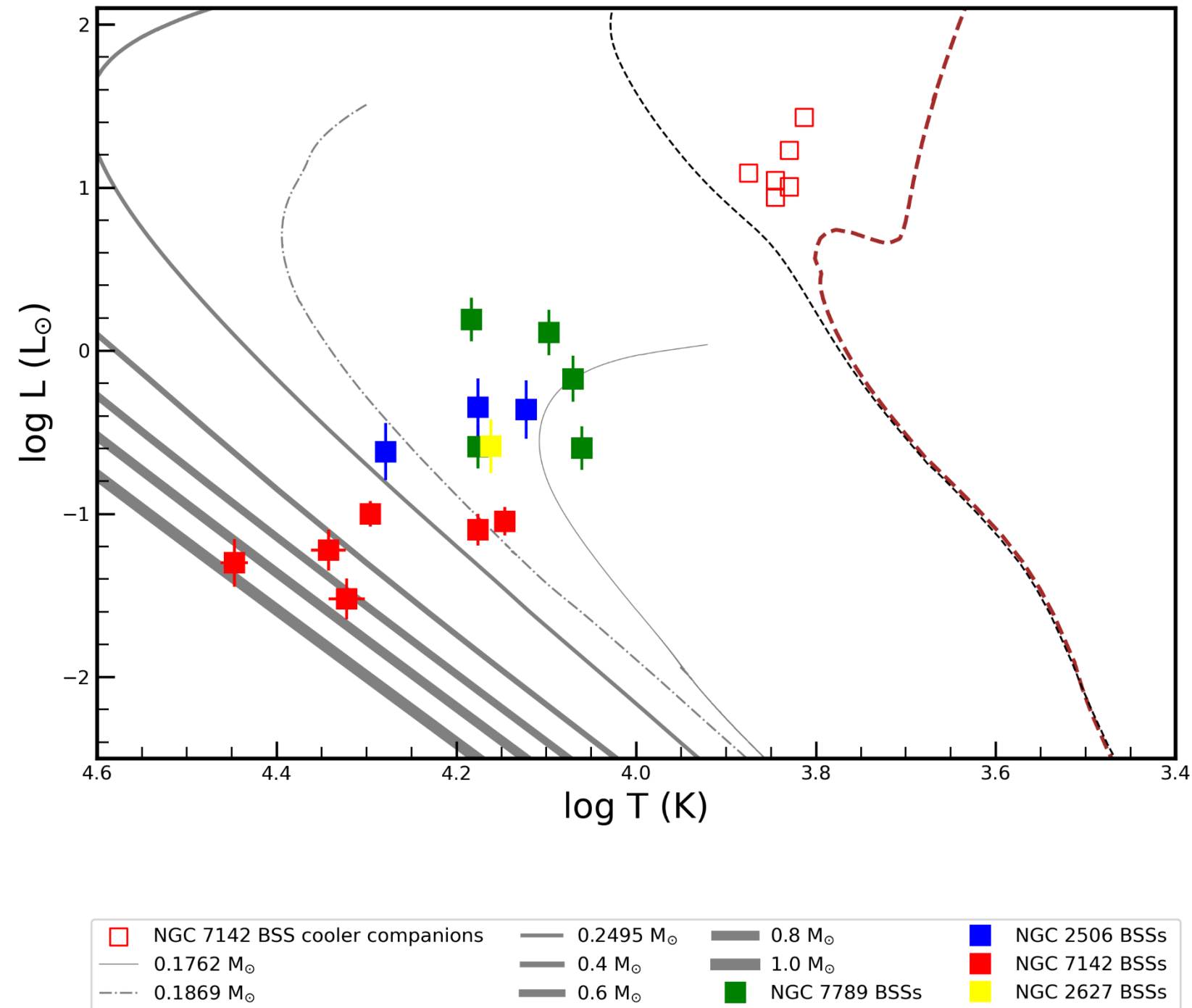
# Hot Companions of BSS and their Properties

---

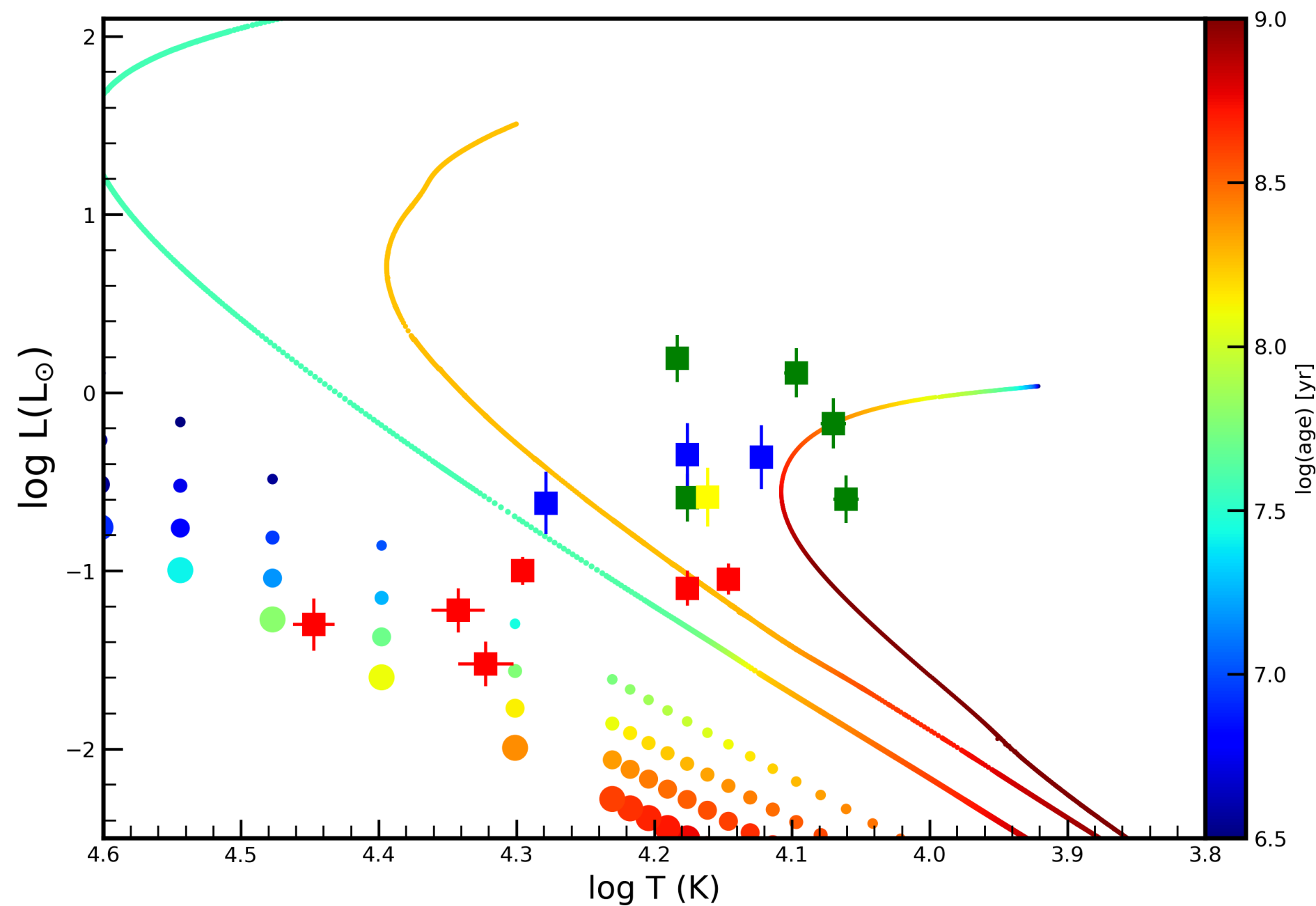
Target	Objects	Temperature (K)	Luminosity ( $L_{\odot}$ )	Radius ( $R_{\odot}$ )
NGC 7789	BSSs	11750 – 15500	0.25 – 1.55	0.069 – 0.242
NGC 2506	BSSs	13250 – 19000	0.24 – 0.44	0.05 – 0.13
NGC 7142	BSSs	14000 – 28000	0.03 – 1.01	0.01 – 0.05
NGC 6940	BSSs	-	-	-
NGC 2627	BSSs	14500	0.26	0.08

---

# Hot components on the H-R Diagram



H-R Diagram showing the PARSEC isochrones fitted to our oldest cluster, NGC 7142. The white dwarf cooling curves of extremely low-mass are taken from Althaus et al. (2013), low-mass are taken from Panei et al. (2007), and normal mass and high mass are taken from Tremblay et al. (2011).



Based on the cooling ages of white dwarfs, the mass transfer in these BSS ended around 10 Myr to 1 Gyr ago.

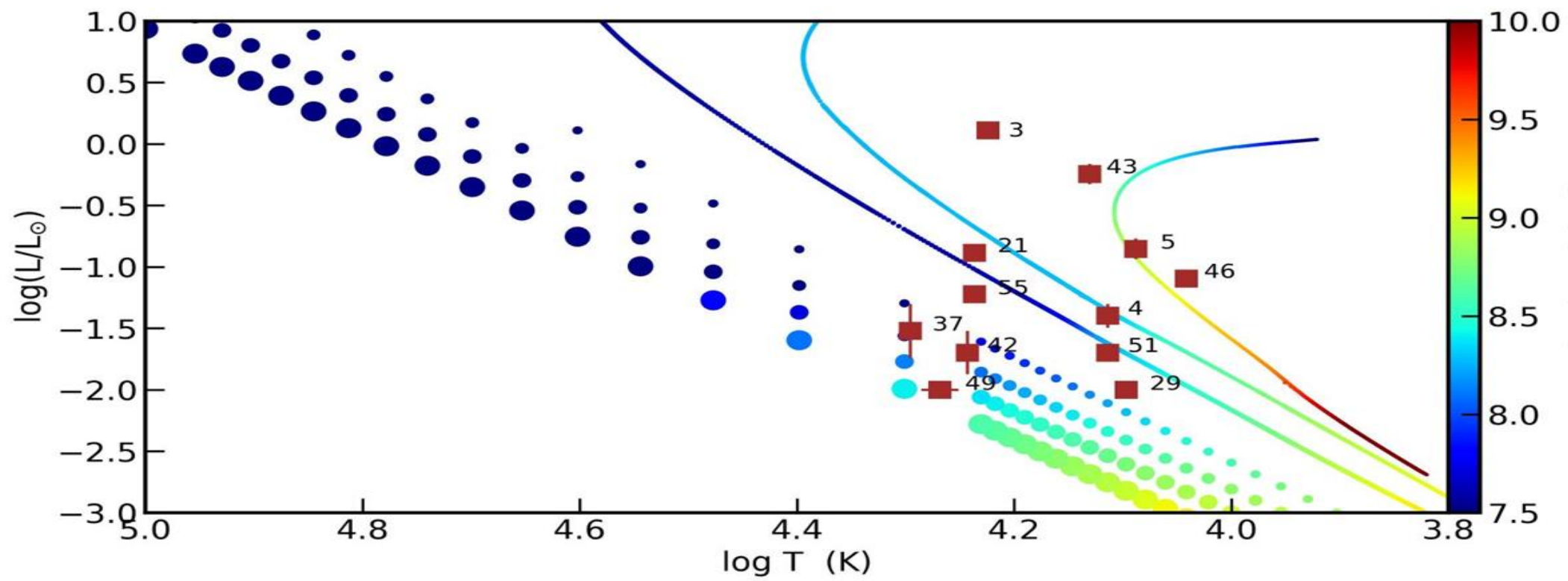
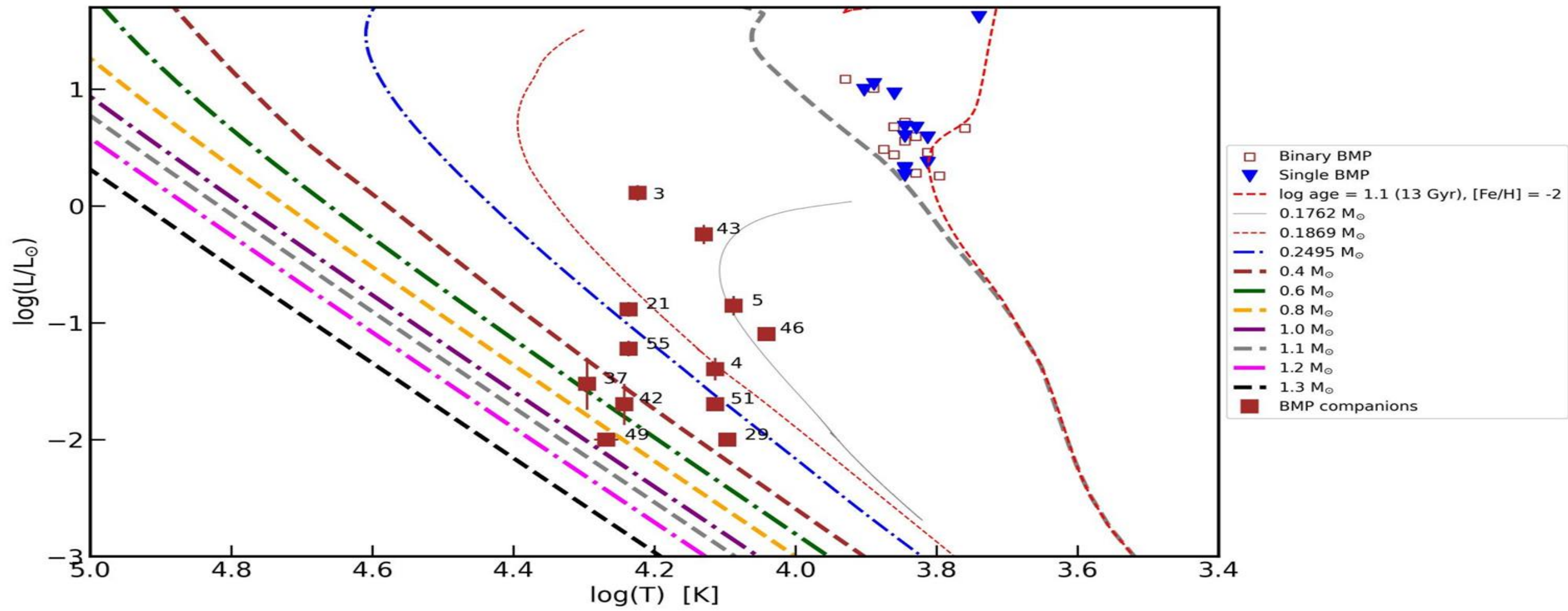
H-R Diagram same as above, but with cooling ages of white dwarfs of different masses shown in the color bar on the right axis.

## Best-fit SED parameters of single BMP stars

		Temperature (K)	Luminosity ( $L_{\odot}$ )	Radius ( $R_{\odot}$ )
Galactic fields	BSSs	5500 – 8000	1.04 – 40.01	0.92 – 7.66

## Best-fit SED parameters of hot companions of BMP stars

		Temperature (K)	Luminosity ( $L_{\odot}$ )	Radius ( $R_{\odot}$ )	Mass ( $M_{\odot}$ )
Galactic fields	BSSs	11000 – 19750	0.01 – 0.57	0.01 – 0.14	0.17 – 0.8




Based on the cooling ages of white dwarfs, the mass transfer in these BSS ended around 30 Myr to 3 Gyr ago.

## Implications on Formation Channels - BSS

- ❖ Total BSS studied – 33
- ❖ **Single-component** SEDs – 15
- ❖ Binary-component SEDs – 15
  - ❖ Extremely low-mass white dwarf companion – 10
  - ❖ Low-mass white dwarf companion – 2
  - ❖ Normal-mass white dwarf companion – 2
  - ❖ Massive white dwarf companion - 1

## Implications on Formation Channels - BSS

- ❖ Total BSS studied – 33
  - ❖ **Single-component** SEDs – 15
  - ❖ Binary-component SEDs – 15
    - ❖ Extremely low-mass white dwarf companion – 10
    - ❖ Low-mass white dwarf companion – 2
    - ❖ Normal-mass white dwarf companion – 2
    - ❖ Massive white dwarf companion – 1
- Case-A/Case-B
- 




# Implications on Formation Channels - BSS

- ❖ Total BSS studied – 33
  - ❖ **Single-component** SEDs – 15
  - ❖ Binary-component SEDs – 15
    - ❖ Extremely low-mass white dwarf companion – 10
    - ❖ Low-mass white dwarf companion – 2
    - ❖ Normal-mass white dwarf companion – 2
    - ❖ Massive white dwarf companion – 1
- Case-A/Case-B
- Case-C
-

## Implications on Formation Channels – BMP

- ❖ Total BMP studied – 27
- ❖ **Single-component** SEDs – 10
- ❖ **Binary-component** SEDs – 12
  - ❖ Extremely low-mass white dwarf companion – 6
  - ❖ Low-mass white dwarf companion – 3
  - ❖ Normal-mass white dwarf companion – 2
  - ❖ Massive white dwarf companion – 1

## Implications on Formation Channels – BMP

- ❖ Total BMP studied – 27
  - ❖ **Single-component** SEDs – 10
  - ❖ **Binary-component** SEDs – 12
    - ❖ Extremely low-mass white dwarf companion – 6
    - ❖ Low-mass white dwarf companion – 3
    - ❖ Normal-mass white dwarf companion – 2
    - ❖ Massive white dwarf companion – 1
- Case-A/Case-B
- 

# Implications on Formation Channels – BMP

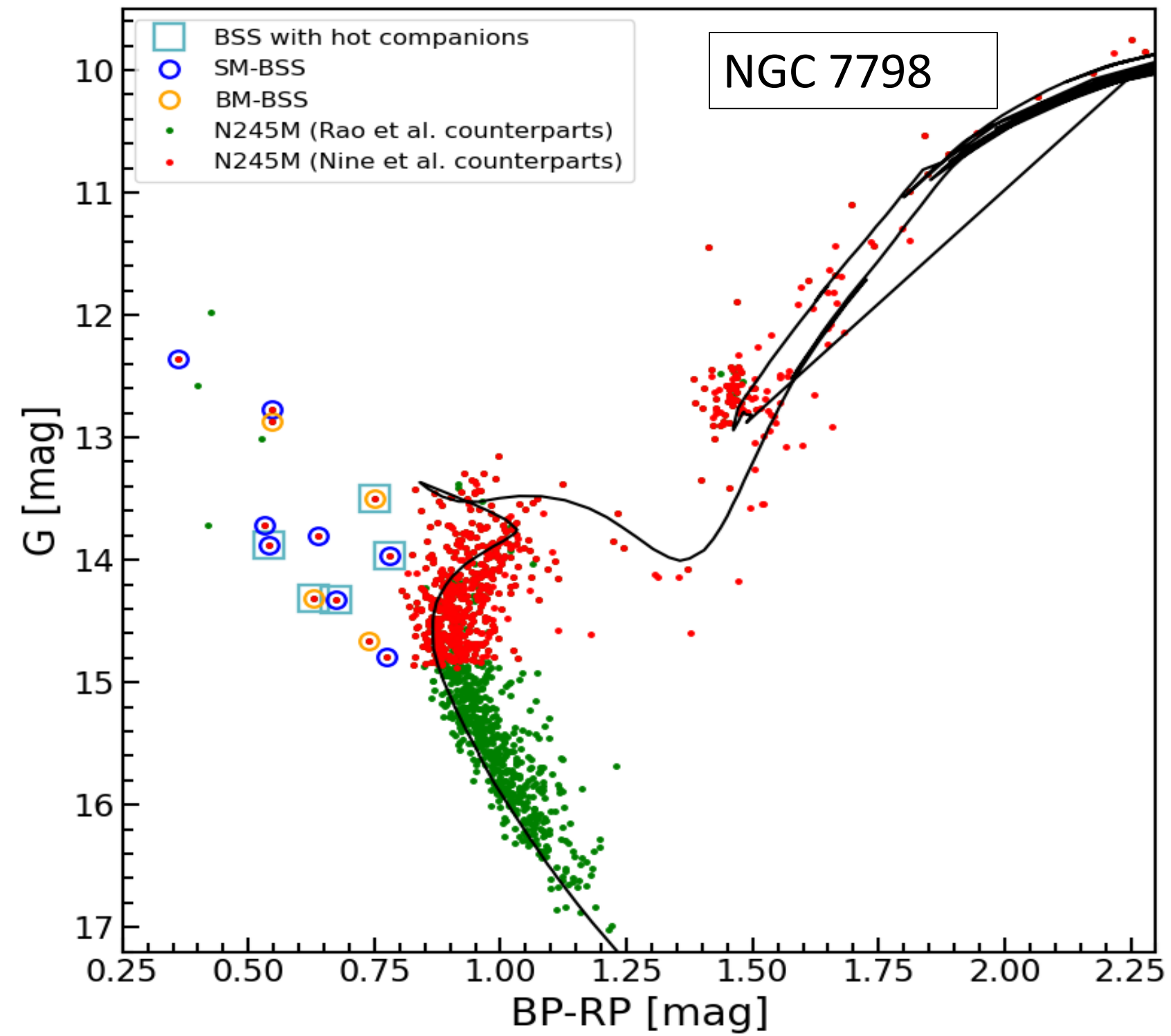
- ❖ Total BMP studied – 27
  - ❖ **Single-component** SEDs – 10
  - ❖ **Binary-component** SEDs – 12
    - ❖ Extremely low-mass white dwarf companion – 6
    - ❖ Low-mass white dwarf companion – 3
    - ❖ Normal-mass white dwarf companion – 2
    - ❖ Massive white dwarf companion – 1
- Case-A/Case-B
- Case-C
- 
- ```
graph LR; A[Extremely low-mass white dwarf companion - 6] --> B[Case-A/Case-B]; C[Low-mass white dwarf companion - 3] --> B; D[Normal-mass white dwarf companion - 2] --> E[Case-C]; F[Massive white dwarf companion - 1] --> E;
```

# CONCLUSION & FUTURE WORK

- ❖ About 45% of BSS, as well as BMP stars, may have formed via mass transfer.
- ❖ Spectroscopic data for abundances and binarity information, and construction of detailed formation histories using MESA or other suitable models would be valuable.

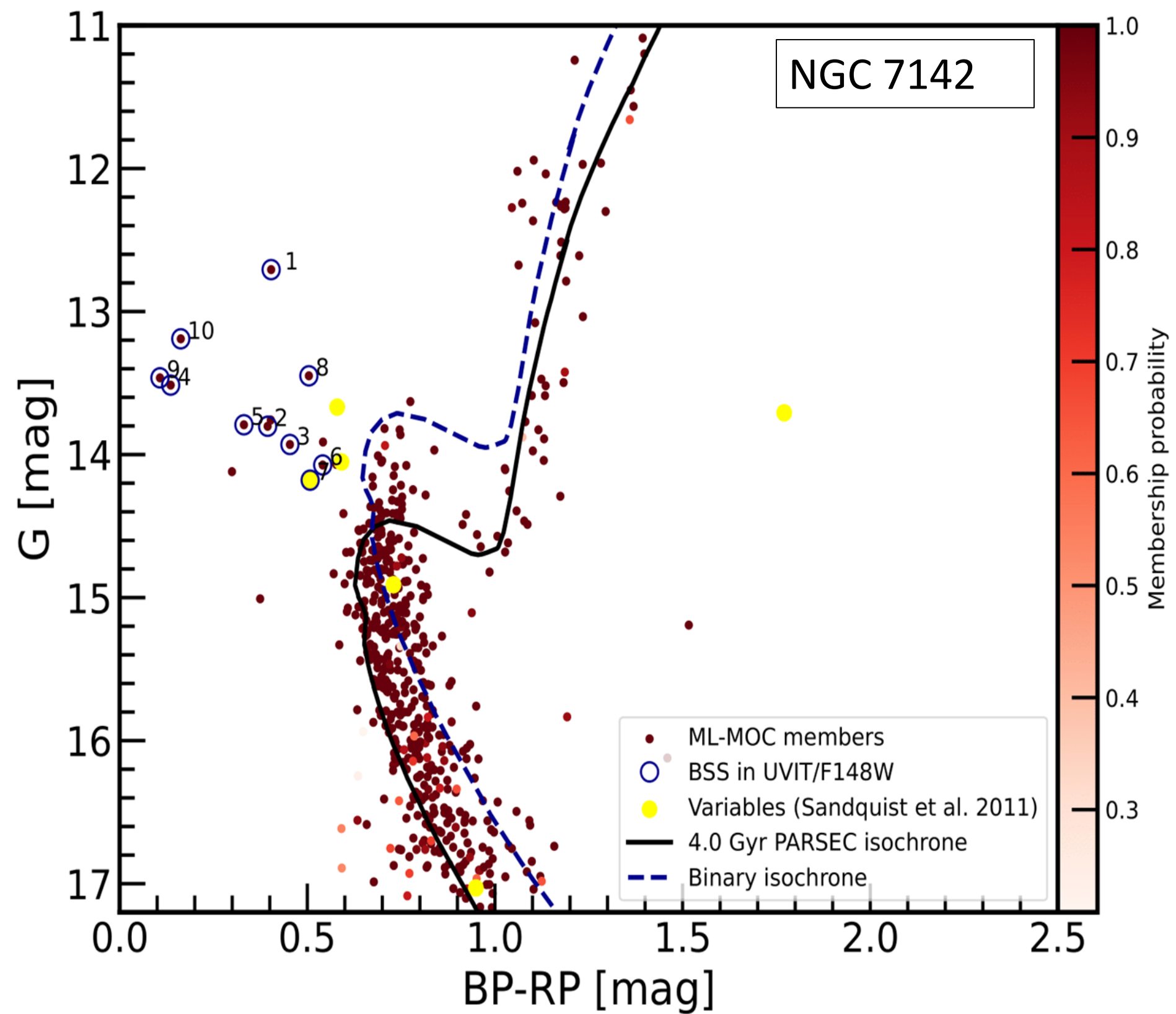
Thank You!!!

**EXTRA SLIDES**

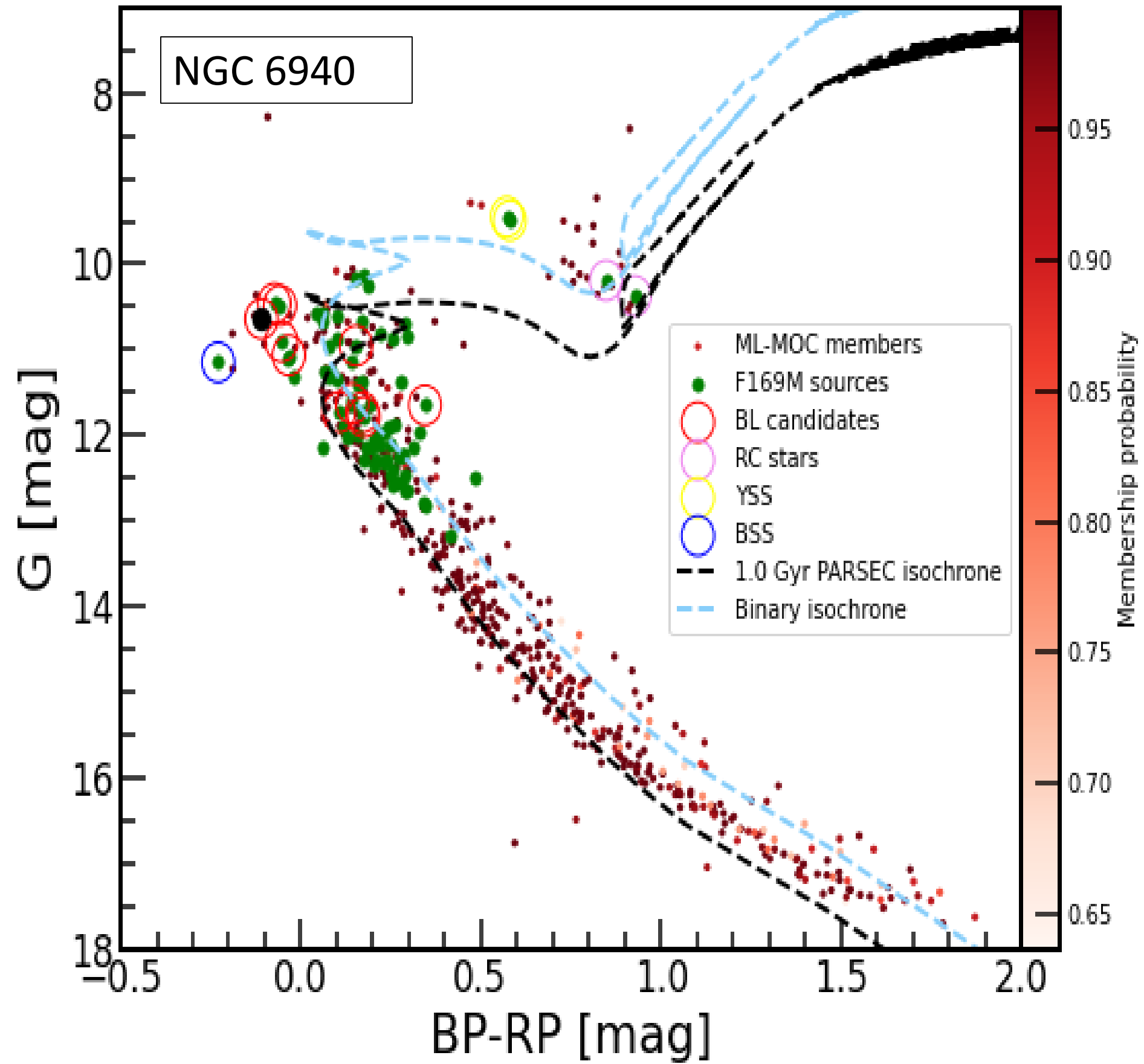


Distance: 2000 pc;  $E(\text{BP-RP}) = 0.375$ ;  $A_G : 0.39$ , Age: 1.6 Gyr





Distance: 2368 pc;  $E(\text{BP-RP}) = 0.03$ ;  $A_G : 0.09$ , Age: 4.0 Gyr



Distance: 2368 pc;  $E(\text{BP-RP}) = 0.03$ ;  $A_G : 0.09$ , Age: 4.0 Gyr

# NGC 7789 – Best-fit parameters of BSS and Hot Companions

| Name  | Component | $\log g$ | $T_{\text{eff}}$<br>[K] | $R$<br>[ $R_{\odot}$ ] | $L$<br>[ $L_{\odot}$ ]    | Scaling factor | $N_{\text{fit}}$ | $\chi_r^2$<br>( $\chi_{r,\text{single}}^2$ ) | $v_{\text{gfb}}$ |
|-------|-----------|----------|-------------------------|------------------------|---------------------------|----------------|------------------|----------------------------------------------|------------------|
| BSS2  | single    | 4.0      | $8750 \pm 125$          | $3.04 \pm 0.152$       | $47.7 \pm 4.81$           | 1.18E-21       | 18               | 286.1                                        | 0.77             |
| BSS3  | single    | 4.0      | $8750 \pm 125$          | $2.09 \pm 0.104$       | $22.4 \pm 2.25$           | 5.46E-22       | 20               | 289.5                                        | 0.51             |
| BSS4  | single    | 4.5      | $8000 \pm 125$          | $2.28 \pm 0.114$       | $19.0 \pm 1.91$           | 6.61E-22       | 20               | 86.7                                         | 0.19             |
| BSS5  | A         | 4        | $8000 \pm 125$          | $1.79 \pm 0.089$       | $11.75 \pm 1.18$          | 4.082E-22      | 13               | 101.0 (500.8)                                | 0.091            |
|       | B         | 9.5      | $15000^{+250}_{-250}$   | $0.075 \pm 0.007$      | $0.258^{+0.093}_{-0.082}$ | 7.213E-25      | –                | –                                            | –                |
| BSS6  | A         | 3.5      | $7250 \pm 125$          | $2.50 \pm 0.125$       | $15.32 \pm 1.54$          | 7.82E-22       | 17               | 67.9 (396.7)                                 | 0.59             |
|       | B         | 9.5      | $11750^{+250}_{-250}$   | $0.197 \pm 0.020$      | $0.672^{+0.255}_{-0.221}$ | 4.98E-24       | –                | –                                            | –                |
| BSS7  | single    | 3.5      | $7500 \pm 125$          | $1.62 \pm 0.081$       | $7.43 \pm 0.74$           | 3.86E-22       | 20               | 278.5                                        | 0.38             |
| BSS8  | A         | 4        | $7750 \pm 125$          | $1.90 \pm 0.094$       | $11.52 \pm 1.16$          | 4.55E-22       | 13               | 79.2 (879)                                   | 0.087            |
|       | B         | 9        | $15500^{+250}_{-250}$   | $0.069 \pm 0.007$      | $0.253^{+0.090}_{-0.080}$ | 6.193E-25      | –                | –                                            | –                |
| BSS9  | single    | 4        | $7500 \pm 125$          | $1.72 \pm 0.086$       | $8.37 \pm 0.84$           | 3.77E-22       | 14               | 79.7                                         | 0.12             |
| BSS10 | A         | 5        | $7250 \pm 125$          | $3.13 \pm 0.156$       | $24.4 \pm 2.45$           | 1.25E-21       | 13               | 143.7 (722.4)                                | 0.53             |
|       | B         | 9.5      | $12500^{+250}_{-250}$   | $0.242 \pm 0.025$      | $1.293^{+0.48}_{-0.42}$   | 7.47E-24       | –                | –                                            | –                |
| BSS11 | A         | 4        | $8250 \pm 125$          | $2.08 \pm 0.104$       | $18.0 \pm 1.82$           | 5.51E-22       | 17               | 110.3 (134.5)                                | 0.089            |
|       | B         | 9.5      | $15250^{+250}_{-250}$   | $0.178 \pm 0.018$      | $1.556^{+0.55}_{-0.49}$   | 4.06E-24       | –                | –                                            | –                |
| BSS12 | single    | 4.5      | $9750 \pm 125$          | $2.99 \pm 0.149$       | $81.6 \pm 8.31$           | 1.14E-21       | 16               | 64.1                                         | 5.12             |
| BSS13 | single    | 4.5      | $8500 \pm 125$          | $2.97 \pm 0.148$       | $42.1 \pm 4.57$           | 1.13E-21       | 20               | 747.5                                        | 3.32             |
| BSS14 | single    | 5        | $10250 \pm 125$         | $3.16 \pm 0.158$       | $102.1 \pm 10.3$          | 1.28E-21       | 16               | 59.1                                         | 1.47             |
| BSS15 | single    | 4.5      | $9500 \pm 125$          | $4.08 \pm 0.204$       | $122.8 \pm 12.3$          | 2.12E-21       | 16               | 47.4                                         | 0.82             |
| BSS16 | single    | 4.5      | $9500 \pm 125$          | $1.84 \pm 0.092$       | $25.0 \pm 2.50$           | 4.29E-22       | 12               | 158.3                                        | 1.08             |

# NGC 2506 – Best-fit parameters of BSS and Hot Companions

| Name | Component | $\log g$ | Luminosity<br>( $L_{\odot}$ ) | $T_{\text{eff}}$<br>(K) | Radius<br>( $R_{\odot}$ ) | $\chi_r^2$<br>( $\chi_{r,\text{single}}^2$ ) | Scaling factor | $N_{\text{fit}}$ | $\text{vgf}_b$<br>( $\text{vgf}_{b,\text{single}}$ ) |
|------|-----------|----------|-------------------------------|-------------------------|---------------------------|----------------------------------------------|----------------|------------------|------------------------------------------------------|
| BSS1 | A         | 3.5      | $31.18 \pm 9.05$              | $7750 \pm 125$          | $3.10 \pm 0.44$           | 308.06 (649)                                 | 5.06E-22       | 16               | 0.15 (0.25)                                          |
|      | B         | 7.5      | $0.44^{+0.22}_{-0.19}$        | $13\,250 \pm 250$       | $0.13 \pm 0.02$           | –                                            | 8.24E-25       | –                | –                                                    |
| BSS2 | A         | 3.0      | $19.30 \pm 5.60$              | $8000 \pm 125$          | $2.29 \pm 0.33$           | 266.26 (694)                                 | 2.77E-22       | 14               | 0.03 (0.16)                                          |
|      | B         | 8.0      | $0.45^{+0.23}_{-0.20}$        | $15\,000 \pm 250$       | $0.10 \pm 0.01$           | –                                            | 5.21E-25       | –                | –                                                    |
| BSS3 | Single    | 4.0      | $31.58 \pm 9.16$              | $9250 \pm 125$          | $2.19 \pm 0.31$           | 48.32                                        | 2.53E-22       | 18               | 0.58                                                 |
| BSS5 | Single    | 4.5      | $84.37 \pm 24.49$             | $9500 \pm 125$          | $3.38 \pm 0.49$           | 13.26                                        | 6.03E-22       | 14               | 0.54                                                 |
| BSS7 | Single    | 4.5      | $18.40 \pm 5.34$              | $9750 \pm 125$          | $1.51 \pm 0.21$           | 68.83                                        | 1.21E-22       | 17               | 0.57                                                 |
| BSS8 | A         | 3.0      | $12.06 \pm 3.50$              | $8250 \pm 125$          | $1.70 \pm 0.24$           | 596.22(1864)                                 | 1.52E-22       | 18               | 0.91 (1.51)                                          |
|      | B         | 7.5      | $0.24^{+0.12}_{-0.11}$        | $19\,000 \pm 250$       | $0.05 \pm 0.01$           | –                                            | 1.19E-25       | –                | –                                                    |
| BSS9 | Single    | 3.0      | $10.58 \pm 3.07$              | $8250 \pm 125$          | $1.60 \pm 0.23$           | 2389                                         | 1.35E-22       | 16               | 1.59                                                 |

# NGC 7142 – Best-fit parameters of BSS and Hot Companions

| Name  | Component | Luminosity<br>[ $L_{\odot}$ ] | $T_{\text{eff}}$<br>[K] | Radius<br>[ $R_{\odot}$ ] | $\chi_r^2$       | Scaling factor | $N_{\text{fit}}$ | $\text{vgf}_b$ |
|-------|-----------|-------------------------------|-------------------------|---------------------------|------------------|----------------|------------------|----------------|
| BSS 1 | A         | $26.97 \pm 0.03$              | $6500 \pm 125$          | $4.09 \pm 0.01$           | 25.11 (211.7)    | 1.51E-21       | 15               | 0.55 (1.94)    |
|       | B         | $0.08^{+0.02}_{-0.01}$        | $15\,000 \pm 125$       | $0.04 \pm 0.0$            | –                | –              | –                | –              |
| BSS 2 | A         | $10.11 \pm 0.01$              | $6750 \pm 125$          | $2.35 \pm 0.00$           | 267.90 (3647.01) | 5.03E-22       | 15               | 0.24 (1.42)    |
|       | B         | $0.05 \pm 0.02$               | $28\,000 \pm 1000$      | $0.01 \pm 0.0$            | –                | –              | –                | –              |
| BSS 3 | A         | $11.00 \pm 0.01$              | $7000 \pm 125$          | $2.25 \pm 0.00$           | 41.74 (111.4)    | 4.62E-22       | 15               | 0.15 (5.11)    |
|       | B         | $0.06^{+0.02}_{-0.01}$        | $22\,000 \pm 1000$      | $0.02 \pm 0.00$           | –                | –              | –                | –              |
| BSS 5 | A         | $12.27 \pm 0.01$              | $7500 \pm 125$          | $2.08 \pm 0.00$           | 159.45 (439.1)   | 3.93E-22       | 15               | 0.25 (2.61)    |
|       | B         | $0.03 \pm 0.01$               | $21\,000 \pm 1000$      | $0.01 \pm 0.00$           | –                | –              | –                | –              |
| BSS 7 | A         | $8.72 \pm 0.01$               | $7000 \pm 125$          | $2.04 \pm 0.07$           | 78.92 (376.08)   | 3.77E-22       | 15               | 0.57 (0.94)    |
|       | B         | $0.1 \pm 0.02$                | $19\,750 \pm 250$       | $0.03 \pm 0.0$            | –                | –              | –                | –              |
| BSS 8 | A         | $16.87 \pm 0.02$              | $6750 \pm 125$          | $3.01 \pm 0.11$           | 38.23 (302.1)    | 8.22E-22       | 15               | 0.12 (2.75)    |
|       | B         | $0.09 \pm 0.02$               | $14\,000 \pm 125$       | $0.05 \pm 0.00$           | –                | –              | –                | –              |

# NGC 6940 – Best-fit parameters of BSS

| Name | Luminosity       | $T_{\text{eff}}$<br>( $L_{\odot}$ ) | Radius<br>(K)   | $\chi_r^2$<br>( $R_{\odot}$ ) | Scaling factor | $N_{\text{fit}}$ | $\text{vgf}_b$ |
|------|------------------|-------------------------------------|-----------------|-------------------------------|----------------|------------------|----------------|
| BSS1 | $32.58 \pm 0.02$ | $8500 \pm 125$                      | $2.63 \pm 0.01$ | 4.21                          | 3.53           | 11               | 0.27           |

# NGC 2627 – Best-fit parameters of BSS and Hot Companions

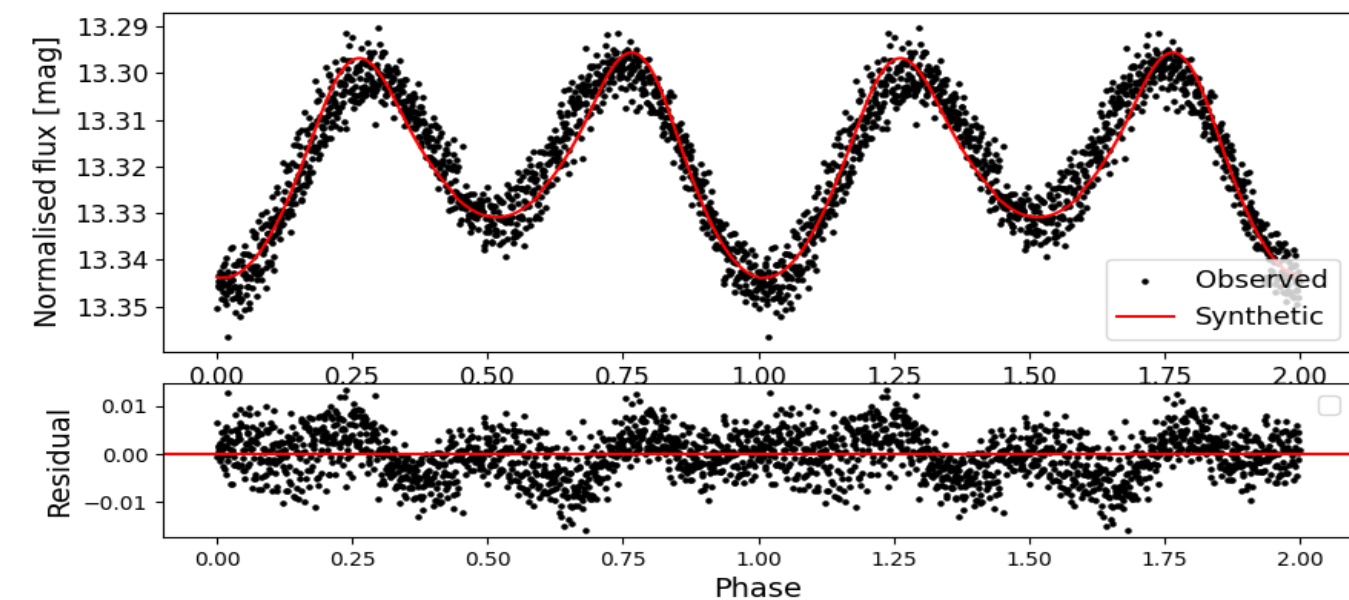
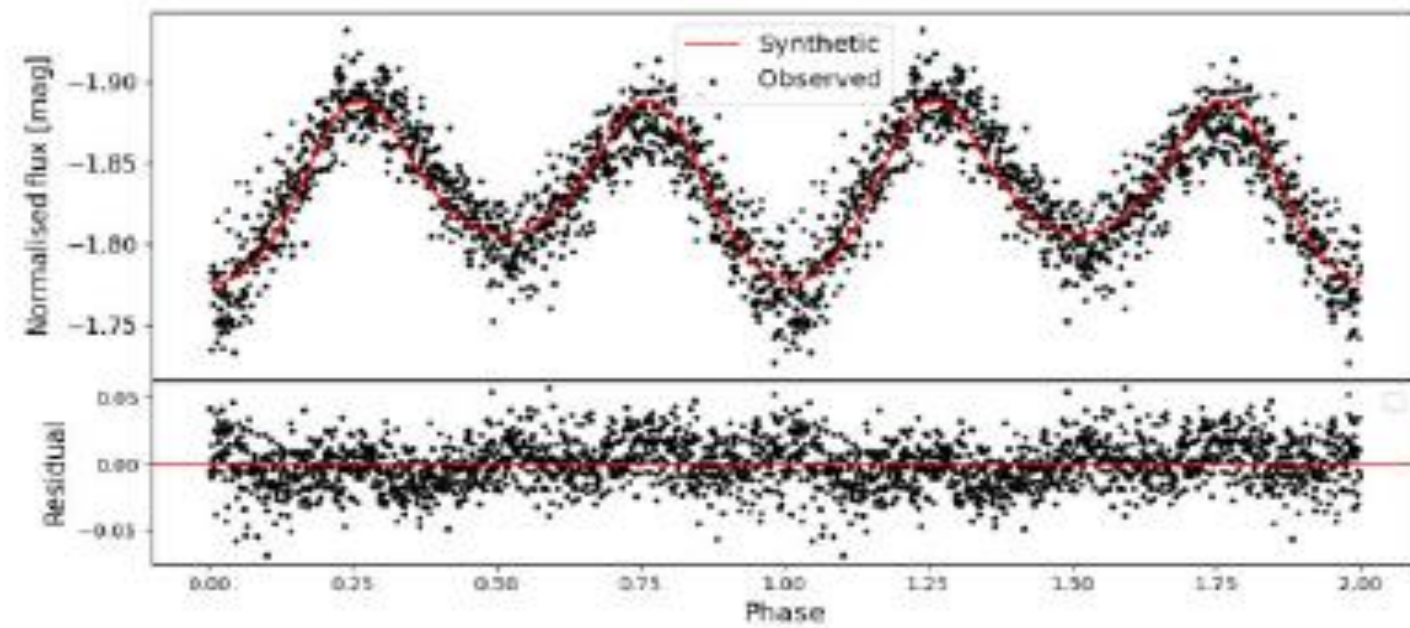
| Name | RA        | DEC       | Component | logg | $T_{eff}$ (K) | L ( $L_{\odot}$ ) | R ( $R_{\odot}$ ) | $\chi_r^2$ | $vgf_b$ |
|------|-----------|-----------|-----------|------|---------------|-------------------|-------------------|------------|---------|
| BSS3 | 129.26101 | -29.83087 | A         | 3.5  | 8000±125      | 10.55±2.99        | 1.69 ± 0.23       | 668.61     | 4.68    |
|      |           |           | B         | 8.5  | 14500±250     | 0.26±0.12         | 0.08 ± 0.01       | 99.94      | 0.81    |

# BMP – Best-fit parameters of field BSS and Hot Companions

| Name  | Component | [L <sub>⊙</sub> ]<br>Luminosity        | [K]<br>T <sub>eff</sub><br>[L <sub>⊙</sub> ] | [R <sub>⊙</sub> ]<br>Radius<br>[K] | χ <sub>r</sub> <sup>2</sup><br>[R <sub>⊙</sub> ] | Scaling factor | N <sub>fit</sub> | <i>v<sub>gfb</sub></i> |
|-------|-----------|----------------------------------------|----------------------------------------------|------------------------------------|--------------------------------------------------|----------------|------------------|------------------------|
| BMP2  | A         | 1.29 ± 0.05                            | 5750 ± 125                                   | 1.14 ± 0.02                        | 14.58                                            | 4.971E-22      | 12               | 0.51                   |
|       | B         | 2.60 ± 0.11                            | 7000 ± 125                                   | 1.09 ± 0.02                        | –                                                | 4.574E-22      | –                | –                      |
| BMP3  | A         | 13.88 ± 0.96                           | 7750 ± 125                                   | 1.69 ± 0.05                        | 79.12 (199.7)                                    | 1.54E-21       | 13               | 0.79 (13.4)            |
|       | B         | 1.29 <sup>+0.21</sup> <sub>-0.19</sub> | 16750 ± 250                                  | 0.14 ± 0.01                        | –                                                | 8.87E-24       | –                | –                      |
| BMP4  | A         | 3.83 ± 0.22                            | 7000 ± 125                                   | 1.33 ± 0.03                        | 54.54 (92.98)                                    | 5.05E-22       | 13               | 2.97 (3.13)            |
|       | B         | 0.04 <sup>+0.01</sup> <sub>-0.01</sub> | 13000 ± 250                                  | 0.04 ± 0.00                        | –                                                | 4.76E-25       | –                | –                      |
| BMP5  | A         | 5.75 ± 0.54                            | 8000 ± 125                                   | 1.24 ± 0.07                        | 157.93 (168.5)                                   | 1.94E-22       | 12               | 3.42 (4.65)            |
|       | B         | 0.14 <sup>+0.03</sup> <sub>-0.03</sub> | 12250 ± 250                                  | 0.08 ± 0.00                        | –                                                | 5.75E-24       | –                | –                      |
| BMP21 | A         | 3.04 ± 0.16                            | 7500 ± 125                                   | 1.03 ± 0.02                        | 13.01 (44.77)                                    | 1.77E-22       | 13               | 1.57 (2.12)            |
|       | B         | 0.13 <sup>+0.02</sup> <sub>-0.02</sub> | 17250 ± 250                                  | 0.04 ± 0.00                        | –                                                | 1.10E-22       | –                | –                      |
| BMP29 | A         | 1.73 ± 0.04                            | 6250 ± 125                                   | 1.12 ± 0.01                        | 5.33 (41.05)                                     | 1.09E-21       | 15               | 0.22 (0.31)            |
|       | B         | 0.01 <sup>+0.01</sup> <sub>-0.00</sub> | 12500 ± 250                                  | 0.02 ± 0.00                        | –                                                | 8.11E-21       | –                | –                      |
| BMP37 | A         | 2.78 ± 0.03                            | 7250 ± 125                                   | 1.05 ± 0.00                        | 40.71 (17.42)                                    | 4.34E-22       | 16               | 0.19 (3.08)            |
|       | B         | 0.03 <sup>+0.02</sup> <sub>-0.01</sub> | 19750 <sup>+1250</sup> <sub>-1000</sub>      | 0.01 ± 0.00                        | –                                                | 8.13E-26       | –                | –                      |
| BMP42 | A         | 2.02 ± 0.15                            | 6750 ± 125                                   | 0.91 ± 0.03                        | 6.18 (91.72)                                     | 3.52E-22       | 20               | 0.15 (2.43)            |
|       | B         | 0.02 <sup>+0.01</sup> <sub>-0.01</sub> | 17500 ± 250                                  | 0.01 ± 0.00                        | –                                                | 6.88E-26       | –                | –                      |
| BMP43 | A         | 11.01 ± 0.45                           | 7750 ± 125                                   | 1.76 ± 0.03                        | 58.39 (133.72)                                   | 2.54E-21       | 14               | 3.67 (7.12)            |
|       | B         | 0.57 <sup>+0.12</sup> <sub>-0.10</sub> | 13500 ± 250                                  | 0.14 ± 0.01                        | –                                                | 1.73E-23       | –                | –                      |
| BMP46 | A         | 3.88 ± 0.08                            | 6750 ± 125                                   | 1.44 ± 0.01                        | 43.46 (108.51)                                   | 2.06E-21       | 15               | 0.4 (5.54)             |
|       | B         | 0.08 <sup>+0.01</sup> <sub>-0.01</sub> | 11000 ± 250                                  | 0.08 ± 0.00                        | –                                                | 5.07E-24       | –                | –                      |
| BMP49 | A         | 2.94 ± 0.04                            | 6750 ± 125                                   | 1.25 ± 0.00                        | 2.31 (47.37)                                     | 1.28E-20       | 10               | 0.12 (3.87)            |
|       | B         | 0.01 <sup>0+.00</sup> <sub>-0.00</sub> | 18500 <sup>+250</sup> <sub>-500</sub>        | 0.01 ± 0.00                        | –                                                | 2.96E-24       | –                | –                      |
| BMP51 | A         | 4.94 ± 0.09                            | 6250 ± 125                                   | 1.92 ± 0.01                        | 150.3 (430.8)                                    | 1.00E-20       | 17               | 0.55 (2.90)            |
|       | B         | 0.02 <sup>+0.00</sup> <sub>-0.00</sub> | 13000 <sup>+250</sup> <sub>-250</sub>        | 0.03 ± 0.00                        | –                                                | 1.27E-20       | –                | –                      |
| BMP55 | A         | 4.75 ± 0.29                            | 7250 ± 125                                   | 1.38 ± 0.04                        | 4.46 (513.43)                                    | 4.20E-22       | 14               | 0.27 (1.87)            |
|       | B         | 0.06 <sup>+0.02</sup> <sub>-0.01</sub> | 17250 <sup>+250</sup> <sub>-500</sub>        | 0.03 ± 0.00                        | –                                                | 1.90E-25       | –                | –                      |



# BSS in Eclipsing Binaries: TESS Light curve Analysis



|        | BSS             |                        | Hot Component                                               |                                                              |
|--------|-----------------|------------------------|-------------------------------------------------------------|--------------------------------------------------------------|
| Object | Temperature (K) | Radius ( $R_{\odot}$ ) | Temperature (K)                                             | Radius ( $R_{\odot}$ )                                       |
| BSS1   | 6000            | $3.55 \pm 0.12$        | $15000 \pm 4500$<br><b><math>15000 \pm 125</math> (SED)</b> | $0.038 \pm 0.011$<br><b><math>0.04 \pm 0.01</math> (SED)</b> |
| BSS7   | 7000            | $5.69 \pm 0.29$        | $20000 \pm 7000$<br><b><math>19750 \pm 250</math> (SED)</b> | $0.037 \pm 0.013$<br><b><math>0.03 \pm 0.01</math> (SED)</b> |

| Nine et al. (2019)                                                                   | Vaidya et al. (2022)                                                                                                            |
|--------------------------------------------------------------------------------------|---------------------------------------------------------------------------------------------------------------------------------|
| ❖ 4 SB1 BSS and 8 single member BSS based on multi-epoch WOCS radial velocity survey | All 12 BSS detected in UVIT NUV filters, and 9 in the FUV filter                                                                |
| ❖ WOCS 20009 (p~ 4190 days, e~0.27)<br>WOCS 10011 (p ~ 517 days, e ~ 0.37)           | WOCS 20009 and WOCS 10011:<br>Extremely low-mass white dwarf companion → Case-A/Case-B.<br>Formation may be in a triple system! |
| ❖ WOCS 5011 (p ~ 2710 days, e ~ 0.67)<br>WOCS 36011 (p ~ 217 days, e ~ 0.54)         | Both fit a single component.<br>White dwarf may be below our detection limit (< 11000 K)                                        |
| ❖ WOCS 25008 – A $\delta$ Scuti variable (p ~0.0955 days, e ~ )                      | Found to have an extremely low-mass white dwarf companion                                                                       |
| ❖ WOCS 27010 and WOCS 15015 are single members                                       | Found with extremely low-mass white dwarf companions Possibly the binaries are having lower inclination angle orbits            |

12 BMP stars fitted with the binary SEDs: FBSS candidates

- **8 are SB1 / binary candidates**
- **3 are RV constants (orbits of these binary systems may be of low inclination)**
- **No information of binarity of remaining 1 BMP star**

10 BMP stars fitted with the single component SEDs : possibly no mass transfer

- **7 are known to be SB1s (WD companion may have cool down)**
- **2 are RV constant stars**
- **1 is a SB2**

## 12 BMP stars fitted with the binary SEDs: FBSS candidates

- **4 enhanced in [Sr/Fe] and [Ba/Fe]**
  - 3 ELM / LM WDs (either intrinsic to the star or acquired in other process before MT)
  - 1 normal mass WD (in agreement with the enhancements)
- **6 deficient in [Sr/Fe] and [Ba/Fe]**
  - 4 ELM / LM WDs (in agreement with the deficiency)
  - 1 normal mass, 1 high mass WD

## 10 BMP stars fitted with the single component SEDs : possibly no mass transfer

- **3 deficient in [Sr/Fe] and [Ba/Fe] (In agreement with the single star)**
- **4 enhanced in [Sr/Fe] and [Ba/Fe] (May be intrinsic to the star)**

# Mass Transfer in a Binary

## Case A

- Compact binary systems ( $p < 10$  days)
- Mass-transfer when primary on main-sequence
- Single massive BSS or short-period binary BSS.

## Case B

- Binary systems ( $p \sim 10$ -500 days)
- Mass-transfer when primary on red giant
- Short period binary BSS with He White Dwarf ( $0.45 M_{\text{sun}}$ ) as a companion

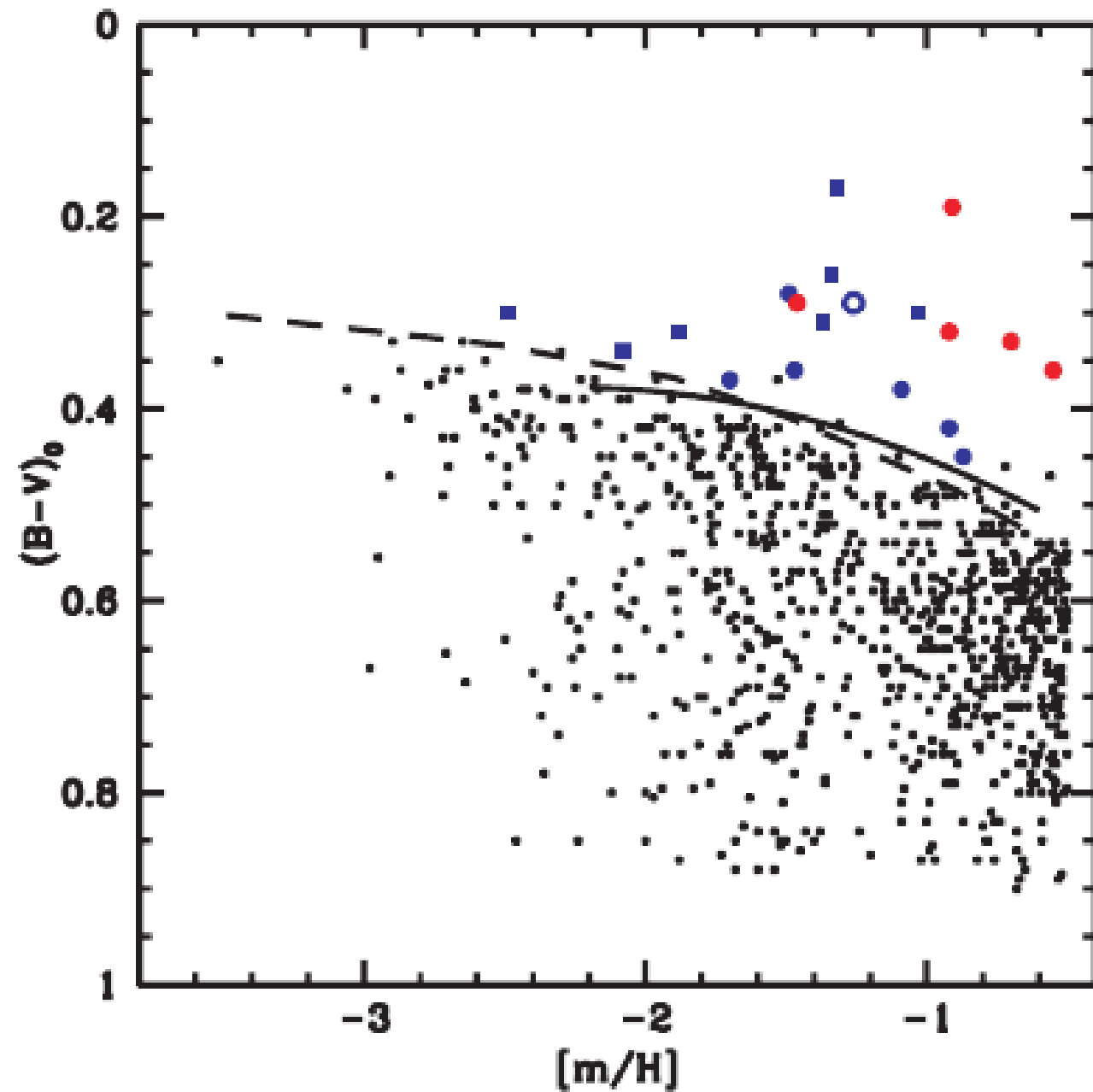
## Case C

- Binary systems ( $p \sim 500$ -2000 days)
- Mass-transfer when primary on asymptotic giant
- Binary BSS with CO White Dwarf ( $0.45 M_{\text{sun}}$ ) as a companion

## Case D

- Binary systems ( $p \sim 1000$ -10000 days)
- Mass-transfer when primary on asymptotic giant
- Binary BSS with CO White Dwarf ( $0.45 M_{\text{sun}}$ ) as a companion

# Field Blue Metal-Poor Stars

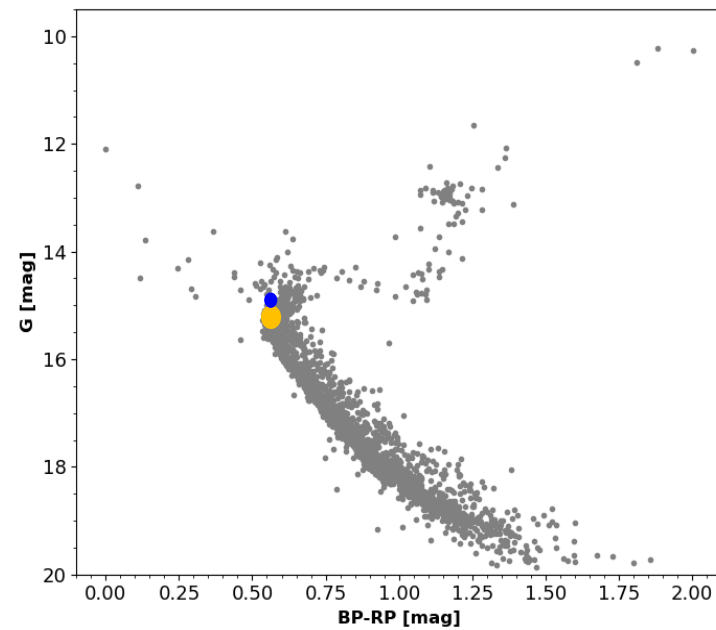


- ❖ Nature controversial – field blue stragglers OR accreted from dwarf satellite galaxy
- ❖ 2/3<sup>rd</sup> of BMP are single-lined spectroscopic binaries (Preston et al. 2000)
- ❖ A fraction also show enhancement in C, Sr, and Ba (Mass transfer)

A color-metallicity diagram from Carney et al. (2005) showing the selection of BMP stars. Solid line shows observed correlation between B-V color and metallicity of globular clusters. Dashed line shows the theoretical relation considering an age of 11 Gyr of clusters.

# Mass Transfer in a Binary

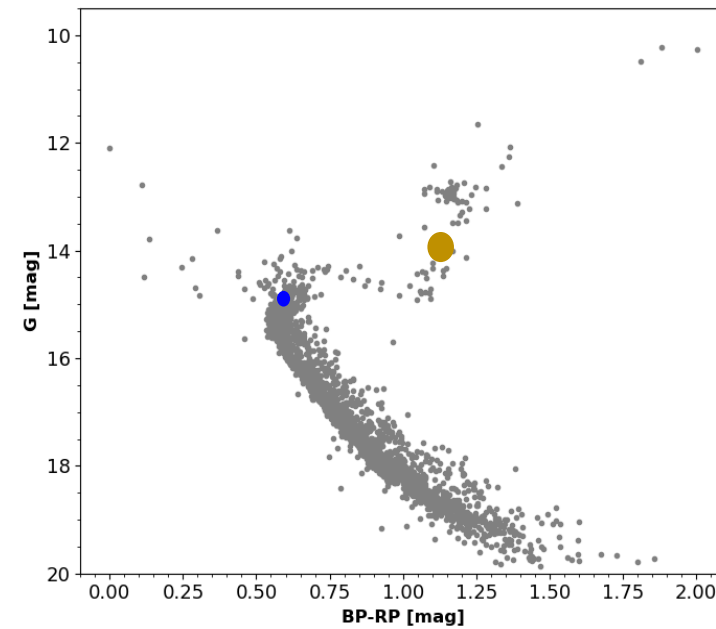
## Case-A



Single massive BSS or short-period binary BSS

Webbink 1976

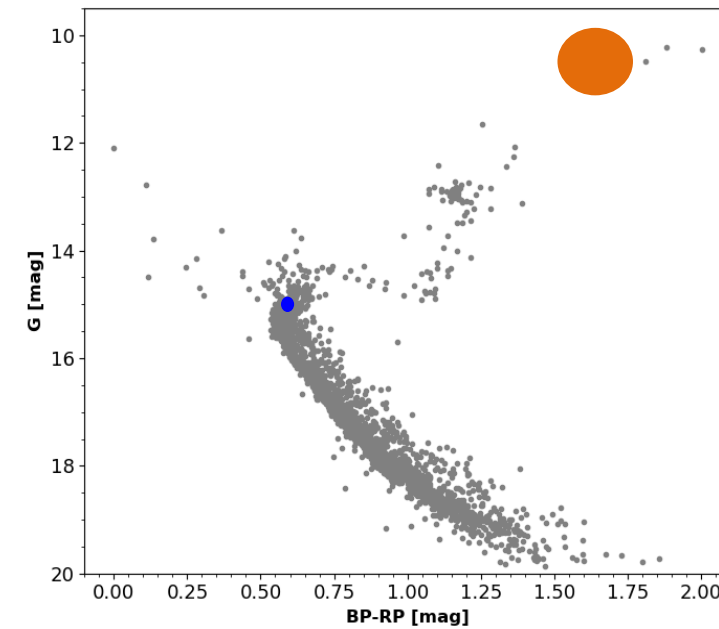
## Case-B



BSS + He core WD ( $M < 0.4 M_{\odot}$ )

McCrea 1964

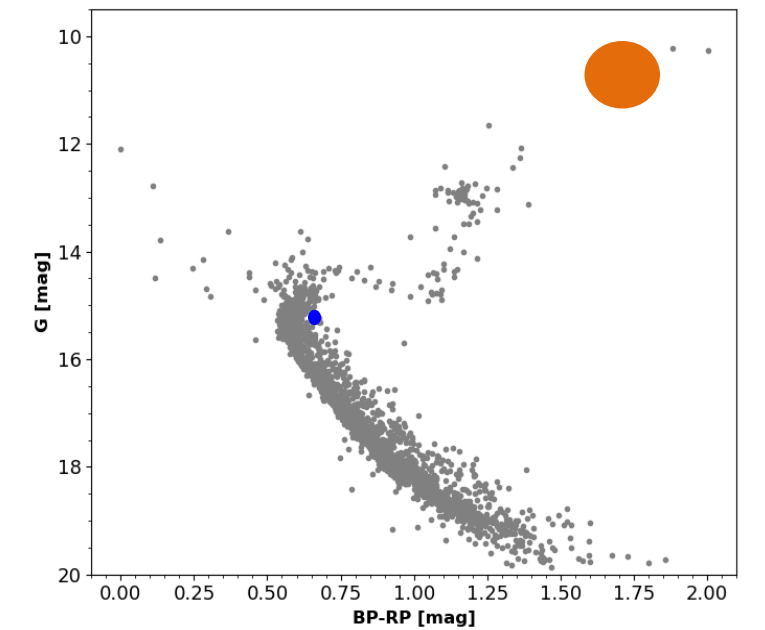
## Case-C



BSS+ CO core WD ( $0.4 M_{\odot} < M < 0.6 M_{\odot}$ )

Chen & Han 2008

## Case-D



BSS+ CO core WD ( $0.4 M_{\odot} < M < 0.6 M_{\odot}$ )

Abate et al. 2013

## BSS SEDs showing UV-excess in Clusters and Fields

| Cluster name    | Single-component SEDs | Excess in UV fluxes | Binary-component SEDs |
|-----------------|-----------------------|---------------------|-----------------------|
| <b>NGC 7789</b> | 8 BSS                 | 7 BSS               | 5 BSS                 |
| <b>NGC 2506</b> | 4 BSS                 | 3 BSS               | 3 BSS                 |
| <b>NGC 7142</b> | 0                     | 7 BSS               | 6 BSS                 |
| <b>NGC 6940</b> | 1 BSS                 | 0                   | 0                     |
| <b>NGC 2627</b> | 2 BSS                 | 2 BSS               | 1 BSS                 |

|                        |        |        |        |
|------------------------|--------|--------|--------|
| <b>Galactic Fields</b> | 10 BMP | 17 BMP | 12 BMP |
|------------------------|--------|--------|--------|